Low-Dimensional Materials
https://www.sciltp.com/journals/ldm

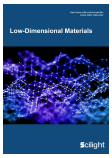

Review

Phonon Engineering in Two-Dimensional Materials for Thermal Devices

Jiawei Li [1], Sikun Chen [2] and Haidong Wang [2,*]

[1] State Key Lab of New Ceramic Materials, School of Materials Science and Engineering, Tsinghua University, Beijing 100084, China
[2] Department of Engineering Mechanics, Tsinghua University, Beijing 100084, China
* Correspondence: hdwang@tsinghua.edu.cn

How To Cite: Li, J.; Chen, S.; Wang, H. Phonon Engineering in Two-Dimensional Materials for Thermal Devices. *Low-Dimensional Materials* **2026**, *2*(1), 3. https://doi.org/10.53941/ldm.2026.100003

Received: 3 March 2026
Revised: 14 March 2026
Accepted: 18 March 2026
Published: 23 March 2026

Abstract: Phonon engineering in two-dimensional (2D) materials provides a method to regulate heat transfer for information processing and thermal management beyond conventional electronics. In 2D materials, phonon spectra, mean free paths (MFPs) and scattering channels can be strongly modified by dimensionality, defects, interfaces and external fields. This review summarizes the thermal conductivity of representative 2D materials, and outlines the main experimental techniques used to measure thermal transport. It then discusses phonon engineering strategies in 2D materials, including asymmetric geometric design, defect engineering and chemical functionalization, van der Waals heterostructures, twist-angle moiré superlattices and external-field or strain-based modulation, highlighting how these approaches reshape phonon transport. The review also surveys thermal devices based on 2D materials, such as thermal rectifiers, thermal transistors, thermal memories and other functional elements for thermoacoustic generation, thermal camouflage and thermal sensing, and compares their operating principles and performance. Finally, this review identifies the remaining challenges for achieving integrated thermal circuits and practical applications, and emphasizes the need for deeper understanding of phonon transport, further optimization of device structures and wider use of data-driven approaches in materials and device design.

Keywords: two-dimensional materials; phonon engineering; thermal conductivity; thermal rectifier; thermal devices

1. Introduction

As the third major energy modulation domain after electronics and photonics, phonon engineering focuses on phonons as the primary subject of study [1]. Phonon engineering means actively controlling the generation, transport, and interactions of lattice vibrations (phonons) in order to manipulate heat flow like electrons, enabling information processing and functional devices [2]. A phonon is the quantized representation of a lattice vibration. Similar to photons, phonons carry the energy and momentum of sound waves [3]. Therefore, the ability to control phonons is of great significance for tuning the intrinsic properties of materials.

Unlike electrons, phonons are bosonic energy carriers and cannot be directly controlled by the polarity of an electric field, which makes it challenging to develop effective methods of phonon regulation [4]. Firstly, electrons obey the quantum-mechanical Schrödinger equation, whereas lattice vibrations follow the classical Newtonian equation of motion; as a result, electrons can occupy positive or negative eigen-energy states, while phonon modes have only non-negative eigen-frequencies. Secondly, electrons possess various atomic orbitals (s, p, d, f), but phonons have only three vibrational polarization directions. Thirdly, electrons are spin-1/2 fermions that obey

Fermi-Dirac statistics, whereas phonons are spin-0 bosons following Bose-Einstein statistics. Electrons carry charge and spin and thus couple directly with electric or magnetic fields, whereas phonons are charge-neutral spinless excitations which makes conventional electromagnetic gating ineffective for phonon control and necessitates alternative modulation methods. However, this simplified distinction does not mean that phonons are always devoid of angular-momentum-related characteristics. Under suitable symmetry conditions, certain phonon modes can possess circular polarization, carry angular momentum, and exhibit chirality [5]. In magnetic systems with broken time-reversal symmetry, phonons may acquire nonzero angular momentum, whereas in nonmagnetic two-dimensional crystals with broken inversion symmetry, phonons at specific high-symmetry points can display definite chirality and pseudoangular momentum [6]. These chiral phonons have been linked to helicity-dependent optical response, intervalley scattering, and symmetry-selective phonon excitation, revealing that phonon regulation can in some cases go beyond conventional control.

Despite these differences, both electrons and phonons in a periodic crystal are described by Bloch wavefunctions, meaning that analogous band-structure engineering principles can be applied to control phonons. In practice, this implies that by designing suitable materials and nanostructures, one can tailor phonon dispersion and scattering to achieve desired functional outcomes. For example, phononic crystals can create phonon band gaps to filter or confine heat-carrying modes, and suitably engineered interfaces or asymmetric structures can produce nonlinear effects such as thermal rectification and transistor-like gating of heat flow.

The rapid development of modern electronic technology has led to serious thermal management challenges because a large fraction of the input energy is dissipated as heat [7]. Phonon engineering aims to convert part of this dissipated heat into a controllable signal and provides a basis for non-electronic information processing [8]. In recent years, advances in nanoscale heat transport have led to the proposal and partial experimental demonstration of thermal logic devices such as thermal diodes [9,10], thermal transistors [11], thermal logic gates [12] and thermal memory elements [13]. These devices are expected to complement conventional electronic components in applications including self-powered computing under extreme conditions and advanced thermal management [14]. As the silicon semiconductor industry approaches scaling limits and the historical trend described by Moore's law slows [15]; phonon-based functions such as thermal rectification offer additional freedom for controlling heat flow in nanoscale devices and can help improve the thermal performance of integrated circuits [16–18].

Two-dimensional (2D) materials, with atomic-scale thickness, provide distinct benefits for phonon engineering [19]. The phonon spectrum of 2D materials has low-dimensional properties, with a flexible out-of-plane acoustic mode, with dispersion relations of acoustic and optical branches that vary from those in bulk materials. The in-plane thermal conductivity of suspended monolayer graphene at room temperature may exceed 3000 W/(m·K) [20]. 2D materials have markedly anisotropic thermal transport characteristics: the in-plane thermal conductivity much surpasses that of the out-of-plane direction, providing them with an inherent advantage for thermal insulation [21]. Moreover, 2D materials possess ultrathin and flexible characteristics, facilitating their transport and integration into heterogeneous systems [22,23]. For example, 2D materials may function as adaptable thermal interface materials for chip cooling, integrating strong thermal conductivity with mechanical flexibility [24]. The varied family of 2D materials provides an extensive array of adjustable thermal characteristics [25]. The low-dimensional phonon properties, anisotropy, and facile integration provide 2D materials an optimal platform for phonon engineering. Analogous to logic components in electrical circuits, thermal logic devices employ the regulation of heat flow to perform comparable purposes, including thermal rectifiers, thermal transistors, thermal logic gates, and thermal memory devices [26]. With the growth of phonon engineering research, the above thermal devices have moved from theoretical models toward actual demonstrations, setting the basis for novel thermal computing and thermal management technologies [27,28]. As summarized in Figure 1, phonon engineering in 2D materials aims to manipulate heat flow using device concepts, including thermal rectifiers, thermal transistors, thermal memories and other thermal devices.

This review has briefly outlined the development of phonon engineering based on 2D materials, focusing on the latest advances in phonon regulation at the 2D scale and the realization of thermal functional devices from theoretical, computational, and experimental perspectives. It also presents an insight on future developments and practical applications of phonon engineering, aiming to broaden researches on phononic devices and logic-thermal circuits.

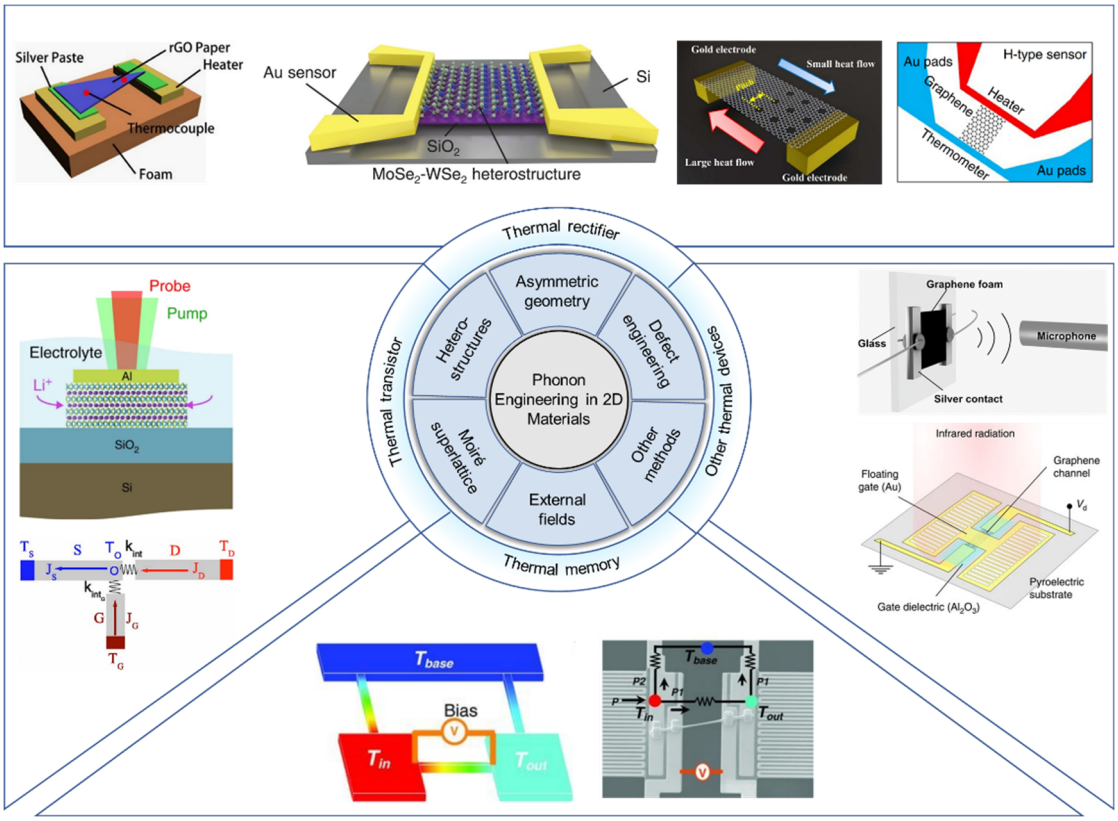

Figure 1. Schematic diagram of the strategies for phonon engineering and thermal devices in 2D materials. Copyright 2012, Springer Nature [29]. Copyright 2022, AAAS [30]. Copyright 2021 IOP Publishing [31]. Copyright 2017, Springer Nature [32]. Copyright 2017, Springer Nature [33]. Copyright 2015, Wiley-VCH [34]. Copyright 2011, Wiley-VCH [35]. Copyright 2008, AIP Publishing [13]. Copyright 2018, Springer Nature [36].

2. Thermal Conductivity of 2D Materials

Phonon-engineering modulation should be reflected through measurable physical quantities, among which the most direct is the thermal conductivity κ, as well as closely related parameters such as interfacial thermal conductance and thermal boundary resistance. Understanding the intrinsic κ of different 2D materials and the factors that govern it helps establish the physical basis of phonon engineering. Compared with studies on electrical, optoelectronic, and catalytic properties, investigations of the thermal properties of 2D materials started relatively late. In thermal transport, the atomic-scale thickness and large specific surface area of 2D materials make surface and interfacial effects particularly pronounced, leading to phonon-transport behavior with strong dimensional effects and anisotropic characteristics. In solids, heat is mainly carried by two types of carriers: electrons and phonons. For most 2D materials, especially intrinsic semiconductors or insulators, the carrier concentration is typically low, and the electronic contribution to thermal conductivity is much smaller than that of phonons. Even in semimetallic materials such as graphene, lattice vibrations remain the dominant heat carriers at room temperature [37]. Therefore, elucidating phonon propagation, scattering, and interactions, and developing phononics-based engineering approaches, are central to understanding and regulating thermal conduction in 2D materials.

The Boltzmann transport equation (BTE) has been successfully employed to investigate phonon-dominated heat transport [38]. Within the BTE framework, the lattice vibrational energy that contributes to thermal transport can be regarded as a phonon gas obeying the Bose-Einstein distribution; accordingly, phonons are treated in a particle-like manner. Due to intrinsic phonon-phonon scattering and scattering by other centers, the phonon distribution function relaxes toward its equilibrium form. Under the relaxation-time approximation, the thermal conductivity of a material can be approximately expressed as:

$$\kappa = -\frac{J}{\partial T / \partial z} = \frac{1}{3} C v l \tag{1}$$

where J is the heat flux density, $\partial T/\partial z$ is the temperature gradient along the z direction, v is the phonon group velocity, C is the phonon volumetric specific heat, and l is the phonon mean free path. Equation (1) provides that

a high thermal conductivity originates from a large specific heat, a high phonon propagation speed, and a long phonon mean free path.

In 2D materials, C and v mainly reflect the intrinsic lattice characteristics and phonon-spectrum structure of a given material, whereas l is highly sensitive to extrinsic factors such as defects, boundaries, interfacial coupling, substrate effects, and interlayer interactions. This relation establishes the physical basis of phonon engineering: practical engineering strategies ultimately operate by tailoring C, v, and l. The phonon spectrum and phonon group velocity of 2D materials exhibit characteristics distinct from those of three-dimensional bulk solids. Because the periodicity of atomic layers is broken along the out-of-plane direction, the in-plane and out-of-plane vibrational modes become more differentiated in their energy and group-velocity distributions, and the out-of-plane branches in the phonon spectrum are softened. Moreover, most 2D materials possess an out-of-plane flexural acoustic branch, whose low-frequency density of states is relatively high and may, under certain conditions, make an important contribution to heat transport [39,40].

Accordingly, we first summarize the intrinsic κ landscape of representative 2D materials, which is primarily governed by their intrinsic phonon spectra. 2D materials exhibit a remarkably wide range of intrinsic κ, which naturally enables them to play different roles in thermal devices. The intrinsic κ of 2D materials spans multiple orders of magnitude: at room temperature, κ can vary from ultrahigh values of >3000 W/(m·K) down to <10 W/(m·K), covering the entire κ range of conventional bulk materials. 2D materials exhibit a huge range of thermal conductivities, which naturally leads to different suitable roles in thermal devices [41]. Carbon-based 2D materials and h-BN typically have high thermal conductivities and are widely regarded as ideal platforms for heat conduction and dissipation [42]. Some transition metal dichalcogenides (TMDCs) and layered halides have κ of <100 W/(m·K), making them more suitable as thermal resistors, thermoelectric materials, or the low-κ side in thermal rectifiers [43].

The primary origin of this exceptionally wide spread in κ lies in the differences in phonon transport. 2D materials with stiff bonding networks and light constituent atoms can sustain phonons with high group velocities, thereby exhibiting ultrahigh in-plane thermal conductivity. In contrast, 2D materials composed of heavier atoms with softer lattices and stronger anharmonicity tend to experience more frequent phonon scattering, which substantially suppresses κ. Structural anisotropy is another important factor: in some layered materials, the lattice exhibits pronounced anisotropy, leading to markedly different thermal conductivities along different crystallographic directions. As shown in Figure 2a, 2D materials can be divided into three categories by different thermal conductivities. The first category is high κ 2D materials whose κ exceeds that of copper. They exhibit heat-transport capability superior to conventional metals, and are represented by graphene [44] and h-BN [45], as well as structurally related systems such as diamane [46] and h-Bas [47]. The second category consists of medium-κ 2D materials with κ between about 10–400 W/(m·K), such as MoS_2 [48] and BP [49], which combine moderate band gaps with intermediate thermal conductivity and are suitable for a variety of functional applications. The third category includes low-κ 2D materials with κ below 10 W/(m·K), whose ultralow thermal conductivities make them attractive for thermoelectric energy conversion and heat-blocking purposes [50–52].

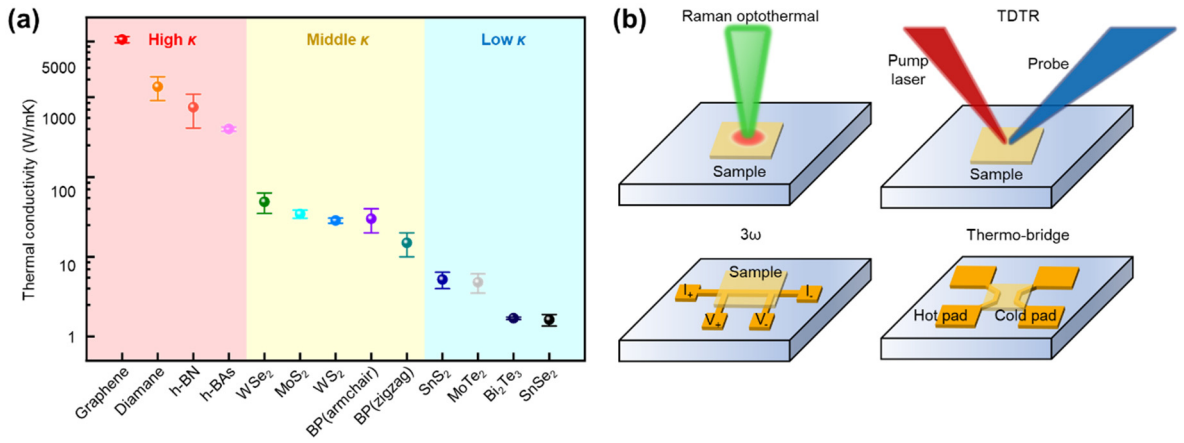

Figure 2. Thermal conductivities of representative 2D materials and commonly used methods for thermal conductivity measurements. (**a**) Range of room-temperature thermal conductivities of representative 2D materials, from ultra-high κ to ultra-low κ systems. (**b**) Techniques for measuring κ in 2D materials: Raman optothermal, TDTR, 3ω and thermo-bridge method.

Thermal conductivity research also provides the methodological basis for subsequent phonon engineering and thermal device design. As shown in Figure 2b, measuring κ in 2D materials is more challenging than in bulk, requiring techniques including thermo-bridge [32,53], 3ω [54,55], Raman optothermal [56–58] and time-domain thermoreflectance (TDTR) [59,60]. Even for the same 2D material, reported κ values often differ by over 50%, due to whether the sample is suspended, the degree of substrate coupling, interfacial thermal resistance, and differing assumptions in data analysis models [61]. Therefore, this section will review κ of representative 2D materials and briefly introduce the main nano-scale measurement methods for thermal conductivity.

Phonon scattering governs phonon transport behavior. In the following, the dominant scattering channels in 2D materials and how they jointly determine l are discussed, giving rise to different transport regimes and providing practical knobs for phonon engineering. Across different length scales, phonons with different scattering mechanisms and MFPs contribute differently to heat conduction, giving rise to distinct transport regimes and enabling diverse phonon-modulation strategies. As illustrated in Figure 3, the MFP is determined by the combined effect of multiple scattering processes. In 2D materials, the dominant mechanisms can be categorized into three types: phonon-phonon scattering, phonon-impurity scattering, and phonon-boundary scattering.

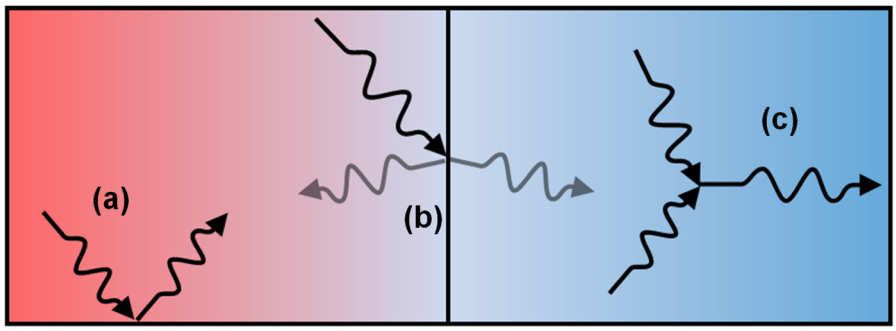

Figure 3. Phonon scattering mechanisms. (**a**) Phonon-boundary scattering; (**b**) Phonon-impurity (dislocation) scattering; (**c**) Phonon-phonon scattering.

Phonon-phonon scattering: This process obeys energy conservation and is commonly classified into Normal processes, in which the total phonon momentum of the system is conserved, and Umklapp processes, which effectively relax phonon momentum. In Umklapp scattering, the phonon momentum can be reversed or substantially changed after the scattering event, leading to a pronounced reduction in the phonon MFP. Because Umklapp scattering introduces thermal resistance, it is the primary mechanism limiting lattice thermal conductivity at elevated temperatures. At high temperatures, when Umklapp processes dominate over other scattering channels, the phonon thermal conductivity can be written as:

$$\kappa = A\frac{M\theta\delta^3 n^{\frac{1}{3}}}{\gamma^2 T} \tag{2}$$

where M is the average atomic mass in the crystal, θ is the Debye temperature, δ is the lattice size, n is the number of atoms per unit cell, and γ is the Grüneisen parameter, and T is the temperature. In 2D materials, stronger anharmonicity corresponds to a larger γ, resulting in a lower phonon thermal conductivity.

Phonon-boundary scattering: For nanoscale samples or few-layer crystals, the phonon MFP is constrained by the lateral size or thickness of the specimen. When the characteristic dimension becomes comparable to the intrinsic MFP, boundary scattering becomes prominent, leading to pronounced size effects in thermal conductivity. Moreover, when a 2D material forms an interface with a substrate or another material, phonons may be scattered at the interface due to acoustic mismatch, interfacial roughness, or weak van der Waals coupling. Such interfacial scattering gives rise to thermal boundary resistance and reduces the effective thermal conductivity.

Phonon-impurity scattering: Point defects (e.g., vacancies and dopant atoms), line defects (e.g., dislocations), as well as microstructural features commonly found in 2D materials such as grain boundaries and wrinkles, can all act as scattering centers. These defects typically scatter high-frequency phonons more strongly. The strength of phonon-impurity scattering is therefore closely tied to material quality; even a small amount of impurities can lead to a substantial suppression of thermal conductivity [62].

In addition to phonon-phonon, boundary, and impurity scattering, phonon lifetimes in 2D materials can also be limited by scattering with electrons. This channel is usually weak in intrinsic or lightly doped semiconducting 2D materials, where lattice thermal transport is dominated by anharmonic phonon-phonon scattering and extrinsic structural scattering. However, when the carrier population is significantly altered by electrostatic gating, chemical

doping, intercalation, or strong photoexcitation, phonon-electron scattering can become an additional channel that shortens phonon lifetimes and modifies the lattice thermal conductivity. Recent work has emphasized that the strength of this effect depends sensitively on carrier density, screening, symmetry, and dimensionality [63].

Phonon-electron scattering should be regarded as a supplementary scattering channel in 2D materials rather than a universally dominant one. Existing studies show that it can be quantitatively important in selected systems. From the viewpoint of phonon engineering, this means that carrier density, electrostatic environment, and nonequilibrium excitation can also be regarded as practical methods for tuning phonon lifetimes in 2D materials [64]. Recent reviews on 2D materials have noted that electron-phonon interaction can significantly affect lattice thermal conductivity in certain materials even near room temperature, especially when carrier concentration becomes sufficiently high [65].

Thermal transport in 2D materials arises from the combined influence of their distinctive phonon spectra and multiple scattering mechanisms. The magnitude of thermal conductivity and its dependence on temperature, thickness, and other parameters are jointly determined by intrinsic anharmonic phonon interactions and extrinsic constraints such as size, layer number, and interfacial coupling. A deep understanding of these microscopic mechanisms provides the theoretical basis for achieving directional and programmable control of thermal conductivity via phonon-engineering strategies.

Reducing a material from a 3D bulk to a 2D thin layer can have complex effects on its thermal conductivity, including two possible trends of enhancement or suppression depending on the material type and the heat transport direction. For example, in terms of in-plane thermal conductivity, different materials show opposite thickness-dependent behaviors: in highly thermally conductive 2D materials like graphene and h-BN, a monolayer's in-plane κ is higher than that of multilayers or the bulk [66,67]. Whereas, for layered materials like $SnSe_2$, thinning down to nanometer thickness significantly reduces κ, which is favorable for insulation and thermoelectric applications [51]. These findings suggest that making a material two-dimensional is itself a powerful phonon engineering approach, which can make high-κ materials even higher and low-κ materials even lower, enabling tuning of thermal conductivity. In addition, the thermal conductivity of 2D materials can be modulated by various external factors. The following are several key factors and representative advances:

Point defects and grain boundaries: Defects are efficient phonon scatterers, so even low concentrations of point defects can strongly reduce thermal conductivity. Simulations show that about 1% carbon vacancies in graphene may already reduce κ by nearly two orders of magnitude [62]. Grain boundaries act as extended defects and likewise enhance scattering; in polycrystalline graphene the thermal conductivity drops sharply as grain size decreases, falling to only a few hundred W/(m·K) when the grains are a few hundred nanometers [68]. Increasing grain size by optimized growth or annealing can restore κ toward the single-crystal limit. Controlling defect concentration and grain size during synthesis is therefore crucial when high thermal conductivity is required [69].

Mechanical stress and strain: Applied stress or strain changes lattice constants and the phonon spectrum and thus affects heat transport. In general, tensile strain softens the lattice and lowers phonon velocities, which reduces thermal conductivity. For graphene and monolayer WS_2, theory and experiment both indicate a clear decrease in κ with increasing tensile strain, with reductions of several tens of percent at moderate strain levels [70,71]. The main reason is enhanced scattering of low-frequency acoustic phonons in the distorted lattice [72]. Non-uniform stress can therefore be used as a reversible and relatively fast way to tune κ, but in flexible devices repeated bending may degrade thermal performance and should be evaluated [51,73].

Substrate coupling and interfacial thermal resistance: Because 2D materials are extremely thin, interfacial thermal resistance has a strong influence on the effective thermal conductivity in supported or stacked structures. At the graphene-SiO_2 interface, phonon spectrum mismatch leads to large thermal resistance and a marked suppression of the measured in-plane κ [74]. Using substrates with smoother interfaces and higher thermal conductivity, such as h-BN, can improve heat spreading; transferring graphene from SiO_2 to h-BN has been shown to significantly increase its room-temperature κ [75]. Similar issues arise at metal-2D interfaces, where poor thermal contact can limit the performance of 2D thermal interface materials. Interface engineering that strengthens phonon coupling, for example through suitable interlayers, is therefore an important element of phonon engineering [76].

External field modulation: External fields provide ways to dynamically tune phonon transport beyond static structural design [73]. Optical excitation can create non-equilibrium phonon populations or resonances and thereby modify heat conduction. Electric fields or currents influence κ through electron-phonon interactions and electrostatic stress; in graphene, gate control of carrier density has been predicted and partly observed to alter phonon scattering [77]. In magnetic 2D materials, a magnetic field can change spin order and spin-phonon coupling and thus adjust thermal transport. Although these effects are mostly at the exploratory stage, external-field control

is regarded as a promising route toward active and reversible phonon-based components such as thermal diodes and transistors [78].

In summary, various external factors provide abundant means to modulate the thermal conductivity of 2D materials. From a materials design perspective, these factors are concrete implementation pathways of phonon engineering. In designing 2D-material-based devices, fully leveraging and combining the above modulation methods can greatly expand the applications of 2D materials in thermal management and thermal functional devices. The mechanisms and effects of each factor differ, and must be balanced against specific application requirements. For example, for scenarios requiring high thermal conductivity, one should minimize impurities/defects, maximize isotopic purity, and choose excellent substrates; whereas when insulation or directional heat flow is needed, one can employ doping/defects or external fields to lower thermal conductivity in specific directions. By optimally combining the above strategies, one can achieve comprehensive control of heat transport performance in 2D materials from the atomic scale to the device scale.

3. Phonon Engineering Methods in 2D Materials

Various approaches to modulating the intrinsic thermal transport of 2D materials provide the foundation for phonon engineering. This section discusses specific strategies for phonon engineering in 2D materials, focusing on how the generation, propagation and scattering of phonons can be controlled through the design of material structure, and outline how these approaches modify phonon transport and support the operation of thermal devices. Phonon engineering in 2D materials can be organized into three conceptually distinct yet complementary routes. (1) Scattering engineering manipulates the phonon MFP spectrum by tuning resistive scattering channels, directly controlling l. (2) Spectrum engineering reshapes phonon dispersion and mode participation, tuning the distribution of v and the spectral weight in C, and often altering selection rules and hybridization. (3) Topological and nonequilibrium engineering targets directionality, robustness, switchability, and nonlinear response, enabling device-level functionalities that cannot be captured by a single scalar κ.

3.1. Scattering Engineering

In most 2D materials at room temperature, the lattice heat capacity does not vary dramatically, and the baseline group velocity is largely fixed by bonding and mass. Therefore, a dominant lever for tuning κ is to engineer the MFP spectrum l by controlling resistive scattering. Microscopically, the total scattering rate can be viewed as a combination of intrinsic anharmonic (Umklapp) scattering and extrinsic channels:

$$l^{-1} = l_{\mathrm{U}}^{-1} + l_{def}^{-1} + l_{bd}^{-1} + l_{int}^{-1} + l_{e}^{-1} \cdots \tag{3}$$

where defects, boundaries, interface, strain-modulated anharmonicity, and electron contribute in mode-dependent manners. Scattering engineering thus offers a direct pathway to reduce κ for thermal devices, or to create spatially asymmetric scattering profiles for rectification.

3.1.1. Asymmetric Geometry Design

Introducing geometric asymmetry in the shape or boundaries of 2D materials is one of the fundamental strategies for controlling phonon transport. Non-equilibrium molecular dynamics simulations first revealed thermal rectification effects in asymmetric graphene nanoribbons such as trapezoidal or triangular shapes: heat flow propagates more easily in the direction where the ribbon gradually narrows, while heat transport in the opposite direction is suppressed [79]. For example, Yang et al. observed a thermal rectification ratio as high as ~350% in a trapezoidal monolayer graphene nanoribbon, whereas a symmetric rectangular nanoribbon of comparable size showed only ~70%, as shown in Figure 4a [80]. The physical mechanism was attributed to the match/mismatch of phonon spectra at the hot and cold ends: when the wide end is the heat source, the phonon power spectra of the atomic layers at both ends overlap strongly, and the broadband phonon modes excited at the wide end can propagate unimpeded. In contrast, when the narrow end is the heat source, a clear mismatch emerges between the phonon spectra in high-frequency and low-frequency ranges, so coherent phonon transport is suppressed [81]. As shown in Figure 4b, subsequent studies expanded the forms of geometric asymmetry, including triangular and trapezoidal nanoribbons in monolayer/bilayer graphene [82], Y-shaped three-branch junctions [83], U-shaped bent structures [84], branched nanoribbons [85], etc. Simulation results showed that a monolayer triangular graphene nanoribbon can achieve ~120% thermal rectification at ~180 K, and with perfect edges the rectification effect diminishes with increasing size but still remains around 25% at tens-of-nanometers scale [79]. Introducing additional degrees of freedom such as multiple layers also has a significant impact: a bilayer graphene Y-junction exhibited better rectification efficiency than the corresponding monolayer structure [80].

Asymmetric structures can break the symmetry of heat conduction, with maximum rectification ratios in simulations reaching several-fold or more [85]. This is because altering the geometry often localizes certain phonon modes or induces an uneven distribution of phonon scattering, thereby producing direction-dependent thermal transport properties.

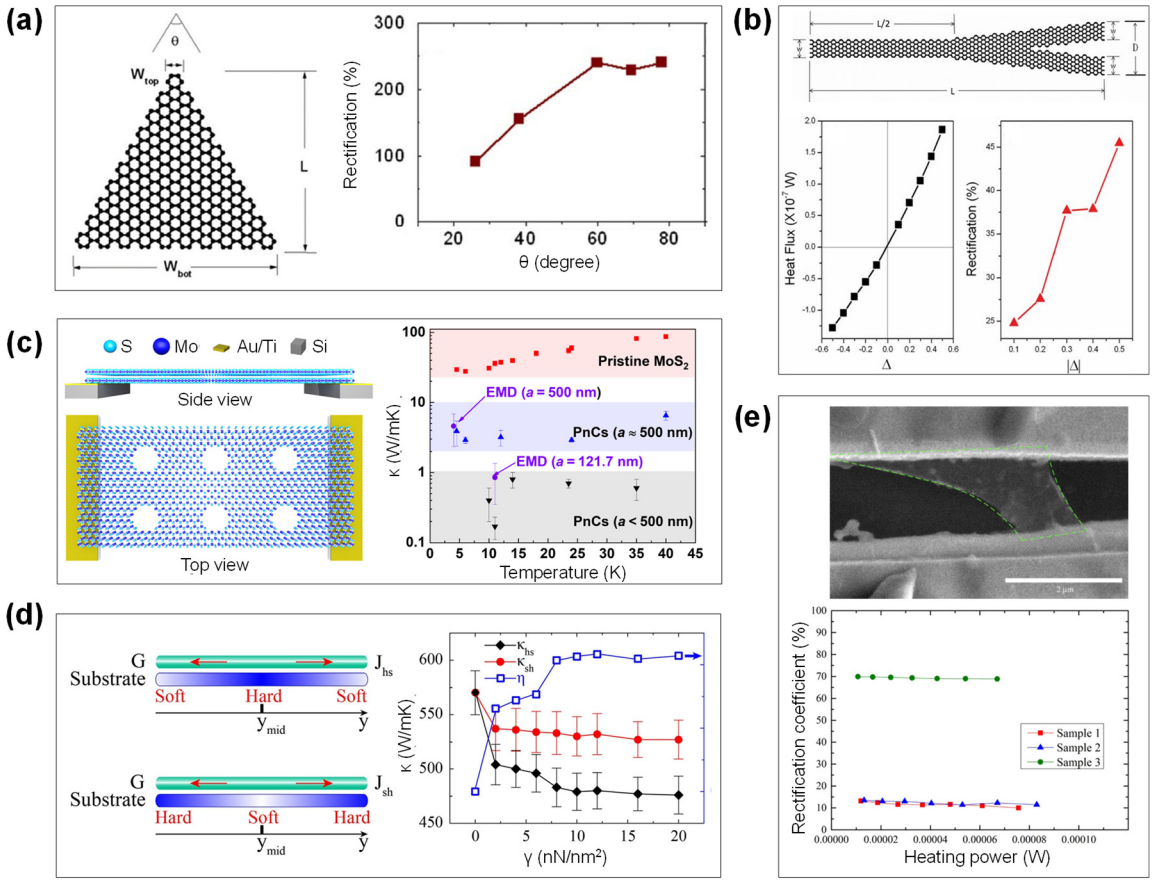

Figure 4. Phonon engineering via asymmetric geometry in 2D materials. (**a**) Schematic of trapezoidal graphene nanoribbons and the corresponding thermal rectification as a function of the opening angle θ. Copyright 2009, AIP Publishing [80]. (**b**) Schematic of a graphene Y-junction, together with the heat flux J versus temperature bias ΔT and the rectification ratio as a function of ΔT. Copyright 2011, Royal Society of Chemistry [83]. (**c**) Side and top views of a few-layer MoS_2 membrane, with a comparison of the experimental κ of the pristine and nanopatterned MoS_2, with the simulated κ. Copyright 2024, AAAS [86]. (**d**) Graphene supported on a substrate with a stiffness gradient, and the effective κ as a function of the stiffness gradient. Copyright 2019, Elsevier [87]. (**e**) SEM images of monolayer MoS_2 samples transferred by PMMA, and the thermal rectification coefficients extracted from the measurements. Copyright 2020 American Chemical Society [88].

Experimentally, micro/nanofabrication techniques have been used to demonstrate proof-of-concept 2D material thermal diodes. In early work, macroscopic reduced graphene oxide (rGO) paper devices were cut into triangular and asymmetric double-rectangular shapes, showing a clear one-way heat flow behavior: in a triangular rGO paper with apex angle 60°, the ratio of forward vs. reverse heating power was 1.28, corresponding to a thermal rectification ratio of ~28% [29]. In suspended monolayer graphene devices, Wang et al. patterned large-area graphene into various asymmetric structures via electron-beam lithography, and used integrated H-type microbridge sensors to precisely measure their thermal transport [32]. The fabricated samples included graphene strips with asymmetric local nanopores and graphene wedges with gradually varying width. These showed an average thermal rectification of ~26% at room temperature. After introducing nanoscale pore defects or geometric tapering on one side did a unidirectional heat-flow difference appear, however, the initial symmetric samples showed no rectification. Beyond graphene, thermal rectification has also been experimentally observed in other 2D materials [89]. In 2020, Yang et al. used focused ion beam cutting to pattern monolayer and multilayer MoS_2 films into asymmetric shapes and measured their in-plane thermal conductivity with suspended microelectrode devices that acted as integrated heaters and thermometers [88]. For three monolayer MoS_2 samples with different geometries, they reported thermal rectification ratios of 10–13%, 11–14% and 69–70%, respectively, as shown in

Figure 4e. These experimental results are consistent with the simulation mechanism: when the wide end is the heat source, the stronger edge scattering at the narrow end makes heat flow more easily from the wide end to the narrow end. In summary, asymmetric geometric design modifies the phonon spectrum and scattering pathways and thus provides an effective means to tune the thermal conductivity of 2D materials, making it one of the most straightforward and widely studied approaches in phonon engineering.

3.1.2. Defect Engineering and Functionalization

By introducing defects such as vacancies, nanopores and grain boundaries, or by adding chemical functional groups into the lattice, phonons can be effectively scattered, which reduces thermal conductivity and can also enable directional control of heat flow. This type of defect engineering exploits the sensitivity of phonons to disruptions of lattice periodicity: impurity atoms and structural imperfections break the coherent propagation of phonons and shorten their mean free paths. Strategies based on doping, vacancies and nanoprecipitates have already been used in 2D thermoelectric materials to enhance performance by strengthening phonon scattering [90]. In 2D materials, functionalization methods such as hydrogenation and nitridation likewise modify bond strength and atomic mass and thus adjust the phonon spectrum. Fully hydrogenated graphene, which effectively introduces light atoms into the lattice, has been shown by experiments and first-principles calculations to have a much lower thermal conductivity than pristine graphene [91,92].

Local functionalization can further be used to construct interfaces with discontinuities in the phonon bands and thereby achieve thermal rectification. Rajabpour et al. simulated graphene-graphane heterojunctions with triangular, T-shaped and other junction geometries and found that differences in the overlap of phonon states on the two sides of the interface are responsible for rectification: when heat flows from graphene to graphane, the reduced overlap of the phonon density of states at the interface hinders cross-interface phonon transport and leads to lower thermal conductivity in that direction [93]. After optimization of the interface angle and size, such partially hydrogenated structures still maintained rectification ratios of about 20–30% at length scales of several tens of nanometers.

Yuan et al. introduced silicon substitutional functionalization at one end of a graphene nanoribbon in another simulation, creating a partially silicon-functionalized region that forms a heterostructure with the pristine graphene [94]. Heat flow then preferentially propagated from the functionalized section toward the pristine section, with a maximum rectification ratio of about 145%, and the rectification strength could be tuned by adjusting the silicon content and its spatial distribution. This behavior was again attributed to differences in phonon spectrum overlap between the two regions: moderate functionalization introduces new localized vibrational modes and reduces the overlap of high- and low-frequency phonon spectra when heat flows in the reverse direction.

Defect engineering has made progress in reducing the thermal conductivity of 2D materials. A recent representative work fabricated MoS_2 films into periodic porous phononic crystal membranes [86]. As shown in Figure 4c, using focused ion beam (FIB) lithography, the researchers etched an ordered nanopore array into a suspended MoS_2 film, and laser Raman thermometry showed its in-plane thermal conductivity to be significantly reduced. Because introducing pores causes relatively little degradation to charge transport, this structure lowered thermal conductivity while still maintaining some electrical conductivity, demonstrating effective thermal isolation and directional heat guiding. This indicates that by nanoscale patterning of the lattice, one can achieve thermal insulation in specific directions in 2D materials. Another experiment used charge injection to tune phonon scattering: Sood et al. reversibly intercalated and extracted lithium ions in an MoS_2 film, finding that its thermal conductivity could be modulated within a certain range [36]. This electrochemical doping effectively introduces point defects and stress fields dynamically, demonstrating the real-time tunability of defect engineering. In summary, defect and functionalization approaches control phonon vibration modes through scattering and localization, and can be used both to reduce thermal conductivity and to direct heat flow. In practical devices, such methods are often combined with geometric design to further enhance rectification ratios or reduce effective thermal conductivity.

3.1.3. Strain Engineering

Stress and strain engineering is another important approach. For suspended 2D materials or those on flexible substrates, local mechanical strain can be used to modify phonon propagation. Molecular dynamics simulations by Gunawardana et al. showed that when tensile stress is applied to one side of a graphene nanoribbon while the other side remains unstressed, heat flows preferentially from the low-stress end toward the high-stress end [95]. In this case, tensile stress increases local phonon frequencies and reduces the effective thermal conductivity on the stressed side, and the resulting difference in lattice constants between the two ends produces a phonon spectrum

mismatch that further suppresses heat transfer in the opposite direction. Experimentally, stress gradients in 2D materials can be created using thermal expansion mismatch or by mechanically bending the substrate, and these gradients have been shown to modulate thermal conductivity. Wei et al. reported thermal rectification in supported graphene induced by modulating the stiffness of the underlying substrate while preserving the structural integrity of the graphene, so that the channel could be reused. As shown in Figure 4d, the heat flux was found to preferentially flow toward the stiffer region of the substrate, and the maximum rectification factor reached about 48% according to an ideal-substrate model [87]. In addition, utilizing nonlinear vibrational states can also alter effective thermal conductivity. For example, in graphene/h-BN heterojunctions, an negative differential thermal resistance (NDTR) phenomenon has been observed, wherein as the temperature gradient increases, the heat flux actually decreases [92].

3.1.4. Phonon-Electron Scattering

Electron scattering can also serve as a supplementary route for phonon engineering in 2D materials. In thermal transport, this process is usually discussed as phonon-electron scattering, while electron-phonon coupling (EPC) provides the broader interaction framework behind it. This route becomes particularly relevant when the electronic subsystem is actively tunable, for example by electrostatic gating, chemical doping, intercalation, or photoexcitation [63]. In such cases, modifying the carrier population changes the available electron-phonon scattering phase space, the electronic screening, and in some systems even the symmetry-allowed coupling channels, thereby altering phonon lifetimes and thermal transport. From the perspective of phonon engineering, the significance of this route lies in its tunability. Unlike static defect introduction, carrier-related scattering can in principle be modulated reversibly through gating, doping, or nonequilibrium excitation [65]. A key advantage of EPC engineering is that it provides access to phonon regulation through electronic control parameters. For example, recent work on graphene heterostructures showed that broken reflection symmetry can activate otherwise restricted electron-flexural-phonon coupling, revealing that interfacial symmetry design can directly tune low-energy EPC [96]. This suggest that EPC engineering may enable active control of phonon transport in ways that are inaccessible through geometry or defect design alone.

EPC engineering can also couple with other phonon-engineering strategies. For instance, strain not only reshapes phonon dispersion, but can also modify the phase space of electron-phonon scattering. In monolayer WS_2, strain was predicted to induce a crossover in nonequilibrium lattice dynamics and activate chiral-phonon emission, illustrating that EPC can serve as a bridge between thermal transport regulation and symmetry-resolved phonon dynamics [97]. Interfacial systems provide another important scenario. In WSe_2/hBN heterostructures, interlayer coupling between hBN out-of-plane modes and WSe_2 out-of-plane modes was shown to enhance the effective electron-phonon interaction in WSe_2 and accelerate electron-hole recombination.[98] From the perspective of phonon engineering, this means that vdWs interfaces can be designed not only to scatter phonons directly, but also to regulate phonon-related functionality indirectly through coupled electron-phonon processes. Such coupling may become relevant for future thermal devices that operate under electrical bias, optical pumping, or multifunctional electro-thermal conditions.

3.2. Spectrum Engineering

Beyond adding scatterers, phonon transport can be engineered by reshaping the phonon spectrum. This route directly influences the distribution of group velocities and the spectral weighting of heat capacity. In 2D materials, spectrum engineering is especially powerful because weak interlayer coupling, twist degrees of freedom, and interfacial interactions can substantially modify phonon modes that dominate heat conduction.

3.2.1. Van der Waals Heterostructures

Using van der Waals forces to assemble different 2D materials into heterostructures can create discontinuities and scattering in the phonon spectrum at interfaces, thereby tuning thermal transport properties. Vertically stacked heterointerface introduces cross-layer phonon scattering and localization. For example, Chiritescu et al. reported an extremely low out-of-plane thermal conductivity (~0.05 W/(m·K)) in disorderedly stacked layered WSe_2 [99]. This is because differences in atomic registry between layers lead to localization of interfacial phonon modes, making thermal vibrations difficult to transmit across layers. Similarly, in graphene/h-BN vertical heterostructures, phonons of different frequencies undergo strong scattering at the interface, causing a pronounced reduction in overall thermal conductivity, and if the interface is engineered to be asymmetric, a thermal rectification effect can be produced [100]. The graphene-WS_2 heterostructure with the lowest cross-plane thermal conductivity is identified by combining Bayesian optimization and molecular dynamics simulations [101]. The results yield an

optimized heterostructure with the lowest thermal conductivity of 0.048 W/(m·K), which is only 5% of the graphite thermal conductivity (Figure 5a). In addition, the 95% reduction is substantial compared to the 50% reduction achieved through modifications in rotation angle, strain, and insertion, demonstrating that the controllability by heterostructure is larger. In one molecular dynamics study, Chen et al. simulated heat transport in a graphene/h-BN heterostructure and found that by constructing a bilayer with top and bottom interfaces of unequal cross-sectional area, a thermal rectification ratio of ~30% could be achieved, as shown in Figure 5b [102]. This was attributed to the difference in acoustic phonon dispersion between the two materials at the interface, which leads to different phonon transmission probabilities in the forward vs. reverse directions [103]. Moreover, in-plane heterojunctions (i.e., stitching different materials within the same plane) also offer new ideas for phonon engineering. For example, Zhang et al. fabricated a lateral monolayer $MoSe_2/WSe_2$ heterojunction, in which heat flows more readily in the direction from $MoSe_2$ to WSe_2, realizing coexisting electrical and thermal rectification within a single atomic layer [30]. This monolayer heterojunction PN diode exhibited a clear diode-like heat conduction asymmetry at room temperature, providing a model for integrated thermo-electronic devices.

Van der Waals heterostructures are particularly promising for thermoelectric energy applications. By introducing multiple interfaces in a 2D material, one can significantly lower the phonon thermal conductivity while keeping the impact on charge transport minimal, thereby achieving a high thermoelectric figure of merit (high ZT). For example, an alternating MoS_2/WS_2 nanoribbon superlattice is predicted to have a ZT at 300 K significantly higher than that of the pure constituents, because interface scattering reduces lattice thermal conductivity while the power factor remains nearly unchanged [104]. A recent review summarized various mechanisms by which 2D heterostructures improve thermoelectric performance, including the synergistic optimization of band engineering and interfacial phonon engineering [105]. In summary, whether in vertical van der Waals stacks or in-plane lattice junctions, heterostructures achieve effective heat-flow control through the phonon discontinuities at material interfaces.

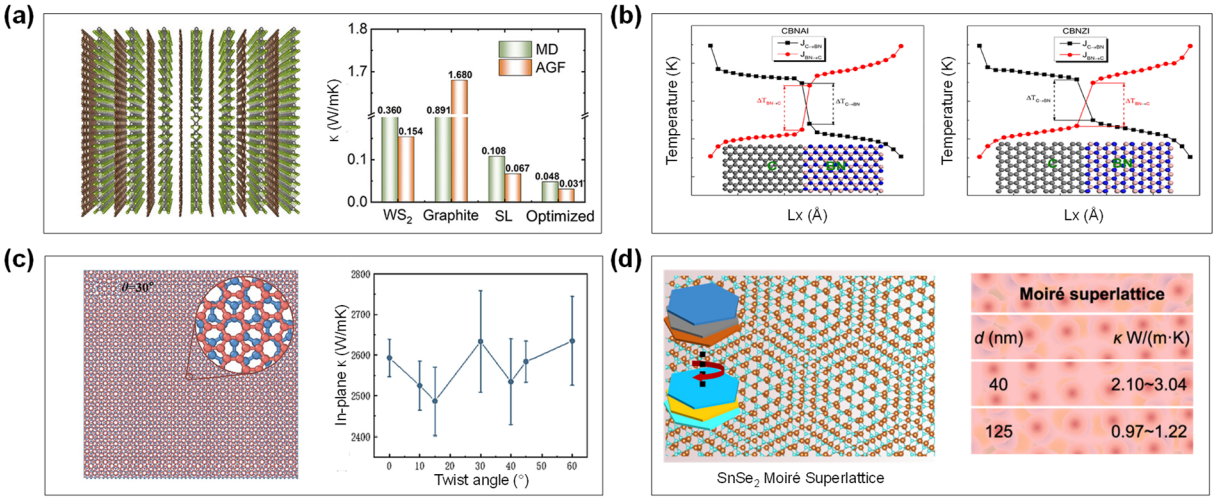

Figure 5. Phonon engineering via defects, heterostructures, moiré superlattice, and stress engineering. (**a**) Structures of the graphene-WS_2 superlattice and thermal conductivities for superlattice and optimized heterostructure. Copyright 2024, American Chemical Society [101]. (**b**) In-plane Gr/h-BN heterostructures with armchair and zigzag interfaces, showing steady-state temperature profiles and interfacial temperature drops under forward and reverse thermal bias. Copyright 2016, Elsevier [102]. (**c**) Bilayer graphene model with twist angles, together with the in-plane κ as a function of twist angle. Copyright 2023, Elsevier [106]. (**d**) Scalable in situ CVD synthesis of twisted multilayer moiré $SnSe_2$ nanosheets, showing markedly reduced thermal conductivity compared with regular multilayer structures. Copyright 2025, American Chemical Society [52].

3.2.2. Moiré Superlattice Modulation

Stacking multiple 2D layers with a specific twist angle creates a moiré-periodic superlattice that induces unique changes in the phonon dispersion, providing a novel approach to modulate thermal conductivity [107,108]. For example, in twisted bilayer graphene, as the relative rotation angle between the two layers varies from 0° to 60°, its in-plane thermal conductivity is not monotonic but reaches a minimum around ~15° and 45°. The thermal conductivity of the bilayer graphene first decreases and then increases with a period of 30° [106]. Simulation studies indicate that at ~15° twist, compared to AB stacking or a fully uncorrelated stacking, the enhanced Umklapp scattering due to interlayer coupling leads to a reduced in-plane thermal conductivity; as the angle

increases further, the interlayer periodicity gradually restores symmetry and the thermal conductivity rises again. Similarly, twisting can significantly affect interlayer heat transport, with the cross-plane thermal conductance reaching a minimum around 30°, as shown in Figure 5c. Notably, at very small twist angles (e.g., the ~1.1° "magic angle"), not only do electronic bands develop flat dispersion and exhibit exotic phenomena like superconductivity, but phonon transport may also become anomalous: one theory predicts a local minimum in thermal conductivity at ~1.08°, thought to be related to low-energy phonon modes in the moiré supercell [109]. The twist angle is a continuously tunable parameter, allowing one to adjust thermal transport properties within the same material system by changing the rotation angle. For instance, one simulation compared the thermal conductivity of single-layer and twisted bilayer graphene at several specific angles, and found that in all twisted cases the bilayer's thermal conductivity was lower than that of both monolayer and AB-stacked bilayer, confirming the general trend that twisting suppresses heat conduction [110]. This is because twisting breaks phonon degeneracies and introduces additional scattering, limiting the effective propagation of long-wavelength phonons. As shown in Figure 5d, the thermal conductivity of the Moiré structure $SnSe_2$ is reduced by approximately 50% compared to the regular structure, despite their similar thickness [52].

Beyond reducing thermal conductivity, moiré superlattices also offer possibilities for directional phonon propagation and band structure engineering. For example, Chen et al. achieved an artificially tuned phonon-polariton spectrum by twisting bilayers of an anisotropic crystal α-MoO_3 [111]. For graphene, a recent experimental work used twist angles to create a phonon "polarizer": researchers measured the anisotropy of heat flow at different twist angles and found that when bilayer graphene is stacked at a specific angle, it can selectively hinder phonons of one polarization from transmitting, thereby controlling the direction of heat flow [112]. Furthermore, emergent phonon modes in moiré superlattices may strengthen interactions with other quasiparticles. One striking example is that superconductivity in twisted bilayer graphene is thought to be related to strong phonon-electron coupling: it has been suggested that low-energy phonons arising in the moiré pattern may act as the mediating glue for electron pairing [113]. From a phonon engineering perspective the twist angle can macroscopically tune the phonon spectrum, thereby affecting the material's thermal conductivity and other physical properties. Looking forward, by varying the twist angle to adjust the lattice thermal conductivity of 2D materials, it may be possible to develop tunable thermal switches and on-demand thermal conductivity structures, providing new design degrees of freedom for thermal management and phononic devices.

3.3. Topological amd Nonequilibrium Engineering

Besides tuning phonon transport through geometry, defects, and interfaces, an emerging route is to engineer the band topology of phonons. In a periodic lattice, phonons are collective excitations with well-defined crystal momentum, and their modes can be organized into bands, similar to electrons. This makes it possible to introduce geometric-phase concepts, such as Berry phase and Berry curvature, into lattice vibrations. The key point is that phonon transport can be controlled not only by scattering and mean free paths, but also by the global band structure and its topology [114]. Moreover, device-level phonon engineering often requires qualitatively new transport features: directional or robust channels, external-field switchability, and nonlinear nonequilibrium response.

3.3.1. Topological Phononics

Topological phononics focuses on designing phonon band structures that host nontrivial topological invariants. When a phonon bandgap carries a nontrivial invariant, boundary-localized modes can appear at edges or at interfaces between two regions with different topology. This is the phononic version of bulk-boundary correspondence [115]. These edge or interface modes are expected to be robust against certain types of disorder, because eliminating them would require closing the bulk gap or changing the invariant. In device language, topology provides a state protection mechanism that is fundamentally different from simply reducing defect density.

A common starting point is the one-dimensional dimerized chain model, which illustrates how band inversion leads to in-gap end states [116]. Although this model is not specific to 2D materials, it sets the conceptual foundation: topology is switched by a parameter that controls the ordering of bands, and the boundary states appear when the system enters the nontrivial phase. In real material design, the parameter can be bond strength modulation, mass contrast, or structural distortion. This logic is directly transferable to 2D lattices.

For two-dimensional systems, the honeycomb lattice is a central platform because it naturally supports Dirac-like crossings in the phonon spectrum. If a symmetry-protected Dirac crossing is gapped by breaking an appropriate symmetry, the gapped bands may become topologically nontrivial. Quantum (anomalous/spin) Hall [Q(A/S)H] states are typical topological states for electrons. Similar states can be realized in phonon systems. A honeycomb lattice is an ideal platform to study the Q(A/S)H-like topological effects of phonons. Its longitudinal

acoustic (LA) and longitudinal optical (LO) branches cross at the BZ corners K and K′, forming a pair of 2D phononic Dirac cones. Figure 6 summarizes a widely used symmetry-breaking framework for 2D honeycomb lattices. In the pristine case, phononic bands can host Dirac-like crossings at the K and K′ valleys, which are protected by the combined crystal symmetries [114]. Once a gap is opened at these Dirac points, the resulting phonon bands may acquire distinct topological characters depending on which symmetry is broken. As illustrated, breaking time-reversal symmetry leads to a QAH-like phase supporting chiral edge modes along the boundary. In contrast, breaking inversion symmetry generates a QVH-like phase with valley-polarized interface states localized at domain walls where the effective mass term changes sign. Introducing a Kekulé-type lattice distortion provides another route to gap the Dirac cones and can yield QSH-like behavior, where pseudospin-momentum-locked boundary transport emerges at interfaces between regions with opposite Kekulé mass. This unified picture highlights a central message of topological phononics: edge or interface phonon channels can be created by engineering symmetry and band inversion, rather than solely by suppressing scattering. Different symmetry-breaking mechanisms lead to different types of topological phonon phases. Breaking time-reversal symmetry can, in principle, produce chiral edge modes, which propagate in one direction and suppress backscattering. Breaking inversion symmetry while keeping time-reversal symmetry can generate valley-contrasting topology, giving valley-polarized interface states at domain walls where the inversion-breaking mass changes sign [117]. In addition, phonons can host pseudospins based on valley, layer, or sublattice degrees of freedom, enabling helical-like boundary transport in appropriately engineered lattices.

Topological concepts are particularly relevant to 2D materials because many of them have hexagonal Brillouin zones and strong valley physics. In such lattices, phonon modes near K and K′ can carry valley-contrasting Berry curvature and exhibit circular polarization, sometimes described as chiral or valley phonons [118]. These features provide practical handles for selective excitation and detection, for example through polarization-resolved optical probes. More importantly for phonon engineering, they suggest that phonon currents can be structured not only by spatial pathways, but also by internal mode labels such as valley or pseudospin.

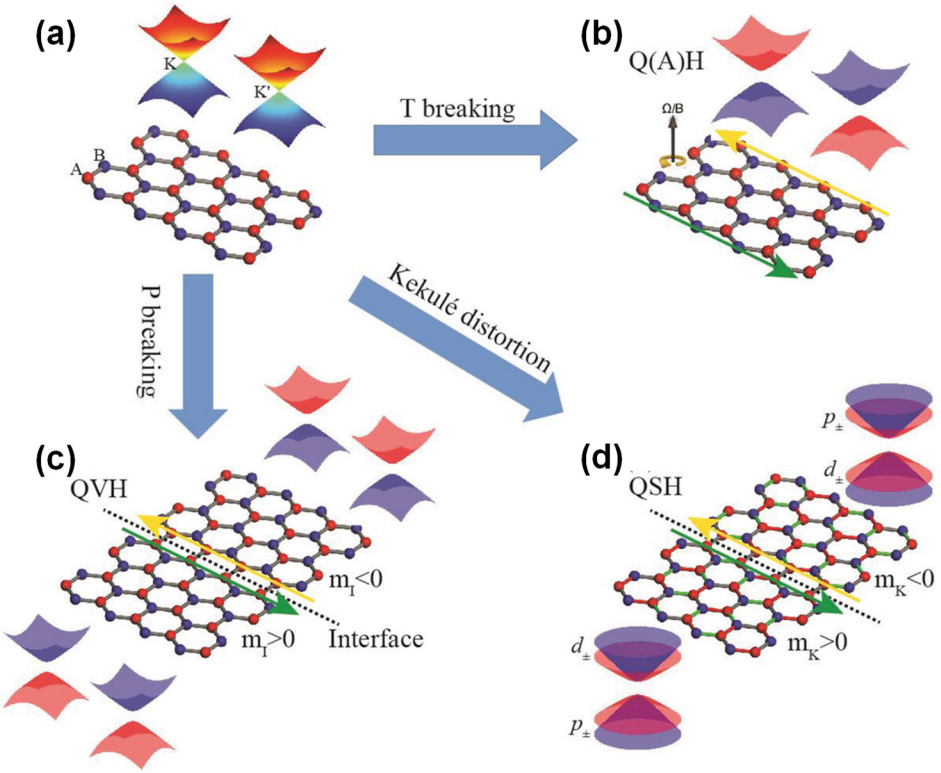

Figure 6. Symmetry-breaking routes to topological phonon phases in a 2D honeycomb lattice. (**a**) Phononic Dirac cones at the K and K′ valleys in a sublattice lattice. Gapping the Dirac spectrum by different symmetry breakings yields distinct topological phonon states: (**b**) time-reversal-symmetry breaking produces chiral edge transport (QAH-like), (**c**) inversion-symmetry breaking produces valley-polarized interface modes (QVH-like), and (**d**) Kekulé distortion opens a gap with pseudospin-momentum-locked boundary modes (QSH-like). Copyright 2019, Wiley-VCH [114].

From the perspective of thermal devices, the most direct implication of topological phononics is the possibility of robust phonon guiding along edges or domain walls [119]. A topological interface can act as a phonon waveguide that routes vibrational energy around bends and imperfections more reliably than conventional waveguides [120]. In principle, one-way edge channels could enable diode-like behavior in multi-terminal geometries [121]. In such a case, the absence of backward-propagating channels would enforce nonreciprocal transport within a certain frequency window. Valley-polarized boundary states suggest a phonon-filtering concept in which only phonons from a selected valley are transmitted. This can be translated into direction-selective routing in designed structures. These ideas provide a complementary strategy to conventional thermal rectification, which typically relies on nonlinearity and spectrum mismatch between two ends.

However, the connection between topological phonon transport and room-temperature heat conduction requires careful discussion. Topological boundary modes are usually defined within a bandgap and occupy a limited frequency range. In contrast, thermal conduction in real 2D materials involves many branches over a wide spectrum and is strongly affected by anharmonic phonon-phonon scattering, especially at elevated temperatures. Therefore, a key challenge is to identify conditions where topological channels make a measurable contribution to net heat flow. Possible directions include designing gaps and boundary modes in thermally populated frequency ranges, enhancing mode selectivity by nanostructuring, and combining topology with nonequilibrium or coherent phonon generation. In this sense, topological phononics is not a replacement for scattering-based phonon engineering, but a higher-level design paradigm that can be integrated with geometry, heterostructures, strain fields, and moiré superlattices to create more controllable and fault-tolerant phonon pathways [122].

3.3.2. Chiral Engineering

In addition to controlling phonon transport through defects, interfaces, strain, and moiré reconstruction, an emerging direction is to engineer phonon chirality. Chiral phonons refer to phonon modes with definite circular polarization and angular-momentum-related character, typically appearing at high-symmetry points or symmetry-preserving paths in momentum space. Earlier studies mainly focused on nonmagnetic two-dimensional hexagonal lattices, where broken inversion symmetry allows phonons at valley points to acquire well-defined chirality and pseudoangular momentum. More recent work has shown that the symmetry conditions for chiral phonons are broader: in two-dimensional lattices with fourfold rotational symmetry, chiral phonons may emerge when time-reversal symmetry is broken, while in three-dimensional chiral tetragonal crystals they can exist along C4-invariant paths even without explicit time-reversal-symmetry breaking [123].

From a phonon-engineering perspective, the significance of chiral phonons lies in the fact that they introduce a symmetry-selective degree of freedom beyond the conventional descriptors of heat transport such as group velocity and mean free path. Because chiral phonons can obey helicity- and momentum-selective excitation rules, they provide a route to manipulate specific phonon branches rather than only changing the overall phonon scattering strength. This feature is particularly attractive in low-dimensional materials, where valley physics, optical selection rules, and interfacial symmetry breaking are already central to electronic and optoelectronic functionality [5]. As a result, chiral-phonon engineering may ultimately connect thermal transport regulation with valleytronic, spintronic, and optoelectronic processes in a unified framework.

Several recent studies suggest concrete pathways for manipulating phonon chirality in low-dimensional systems. For example, theoretical work has shown that strain can substantially modify the phase space of electron-phonon scattering and even activate chiral-phonon emission in monolayer WS_2 under photoexcitation [97]. Interlayer-sliding ferroelectricity in multilayer transition-metal dichalcogenides has also been proposed as a means to tune phonon chirality and phonon Berry curvature through stacking-dependent symmetry breaking. In addition, first-principles screening of two-dimensional transition-metal monocarbides has identified stable monolayers that simultaneously host topological and chiral phonons, indicating that chirality can be embedded into material design rather than treated only as a secondary excitation effect [6]. These studies suggest that chiral-phonon engineering may become a realistic extension of phonon engineering through symmetry design, strain control, magnetic order, and interlayer configuration.

At present, the direct influence of chiral phonons on macroscopic thermal conductivity or thermal rectification in 2D materials is still less established than that of defect scattering, boundary scattering, or interfacial coupling. Nevertheless, chiral phonons are highly relevant to coupled transport scenarios involving optical pumping, valley-selective carrier dynamics, spin-phonon interaction, and nonequilibrium phonon populations. Therefore, although this direction remains at an early stage, it represents a promising frontier in which phonon engineering may evolve from tuning average heat flow to selectively addressing symmetry-resolved phonon modes and their coupled functionalities.

3.3.3. External Fields

Apart from the above strategies, external fields, stress tuning, and non-equilibrium vibrations are also gradually showing potential for modulating phonon transport in 2D materials. In terms of external fields, using electric, magnetic, thermal, etc., fields to influence phonon scattering and spectral distribution is an emerging direction. For example, by applying an electric field or electrochemical bias to change a material's carrier concentration, one can enhance phonon-carrier scattering and lower lattice thermal conductivity. In the experiment by Lu et al. on the perovskite oxide $SrCoO_{2.5}$, they electrochemically inserted/extracted oxygen and hydrogen, realizing bidirectional modulation of thermal conductivity at room temperature by up to an order of magnitude [124]. This shows that external fields can be used to significantly alter lattice vibrational characteristics. Similarly, an applied magnetic field can serve as a phonon engineering tool. In materials with spin-lattice coupling, a magnetic field can change the spin order and magnon spectrum, thereby affecting phonon scattering selection rules. Zhang et al. used a magnetic field to break the symmetry of lattice heat transport and achieve a thermal rectification effect [78]. In that experiment, by tuning the magnetic domain structure, heat flow scattering was made stronger in one direction than the reverse, producing a one-way heat flow. Such magneto-phononic thermal diodes provide a new concept for externally-driven thermal logic devices.

In summary, a variety of techniques, including external fields, electrochemical stress, mechanical strain, and non-equilibrium phonon excitation, are enriching the phonon engineering methods for 2D materials. These methods offer fast, reversible, and spatially selective control, helping compensate for the limited flexibility of static structural designs. Combining these modulation approaches or optimizing them alongside electronic and photonic controls, could enable more efficient and intelligent thermal management devices.

4. Thermal Devices Based on 2D Materials

2D materials, with their atomic-scale thickness, pronounced anisotropy and ease of integration, offer distinct advantages for building thermal devices. In recent years, a variety of phononic thermal devices based on graphene, transition metal dichalcogenides and other 2D materials have been proposed and, in some cases, experimentally demonstrated, including thermal rectifiers, thermal transistors, thermal memories and related functional elements. This section reviews representative advances in these devices, focusing on their structures, material systems, operating principles and performance.

4.1. Thermal Rectifier

A thermal rectifier is one of the earliest widely discussed concepts in 2D thermal devices and aims to achieve directional selectivity of heat flow analogous to an electrical rectifying diode. To realize thermal rectification in 2D materials, researchers have designed a variety of asymmetric structures, such as nanoribbons with asymmetric shapes, heterojunctions and structures with uneven defect distributions [125]. In early work, Yang et al. used non-equilibrium molecular dynamics simulations to show that a trapezoidal graphene nanoribbon can exhibit pronounced thermal rectification: when heat flows from the narrow end toward the wide end, the effective thermal conductivity is significantly reduced [80]. Further studies found that increasing the degree of shape asymmetry, for example by enlarging the trapezoid's top angle, enhances rectification, while increasing the nanoribbon length weakens the rectification ratio [126]. In addition, asymmetric Y-shaped, branched and other three-terminal graphene structures have also been proposed for thermal rectification. Another class of design introduces internal asymmetry, such as periodic voids or mass loading on one side of the material. Hu et al. simulated edge roughness in triangular and trapezoidal graphene nanoribbons, in both single-layer and bilayer forms, and found that with perfectly smooth edges the rectification effect diminishes with increasing size, but at a length scale of about 23 nm it still remains at about 25%; with edge defects, the rectification ratio stabilizes around 30% even for larger sizes [79,127]. These theoretical works demonstrate that asymmetric design of geometry, layer number and defects can produce significant unidirectional heat transport in 2D materials.

The physical mechanisms of 2D thermal rectification usually originate from nonlinear phonon transport, namely the dependence of thermal conductivity on temperature and on the direction of heat flow. In the trapezoidal graphene example, the narrow end at high temperature produces stronger edge scattering and suppresses high-frequency phonon propagation, so heat transfer is impeded when heat flows from the narrow end to the wide end, whereas scattering is weaker in the opposite direction. This symmetry breaking causes the effective thermal conductivity to be lower when the narrow end is on the hot side than in the reverse case, giving rise to rectification. When the sample size is increased such that the phonon mean free path becomes much smaller than the characteristic dimensions of the trapezoidal geometry, this end-contact effect is weakened and the rectification ratio tends to vanish [128]. Besides geometric scattering, phonon spectrum mismatch at heterointerfaces is another

important mechanism. In 1936, a Cu/Cu_2O interface was already observed to exhibit direction-dependent thermal conductance [129]. In 2D materials, a recent experiment achieved a high rectification ratio using a lateral heterojunction: in a monolayer $MoSe_2$/WSe_2 lateral heterostructure, the different temperature dependence of the thermal conductivities of the two materials leads to a preferential heat dissipation path from the $MoSe_2$ side to the WSe_2 side under a large thermal bias, yielding a thermal rectification factor of up to about 96%, as shown in Figure 7a [30]. This result indicates that by selecting and combining 2D materials with contrasting heat transport characteristics, it is possible to approach one-way heat transport at room temperature. Asymmetry in defects or functional groups provides yet another mechanism. Molecular dynamics simulations explained that when the defective or nanoparticle-decorated region is at the hot end, it acts as a phonon bottleneck, limiting the number of phonons reaching the cold end and thus reducing heat conduction in that direction; when the defective region is at the cold end, its influence on overall heat transfer is weaker. In summary, whether asymmetry is introduced through shape, interface or defects, it leads to a direction dependence of thermal conductivity by changing phonon scattering and the phonon spectrum, and thereby produces rectification [130].

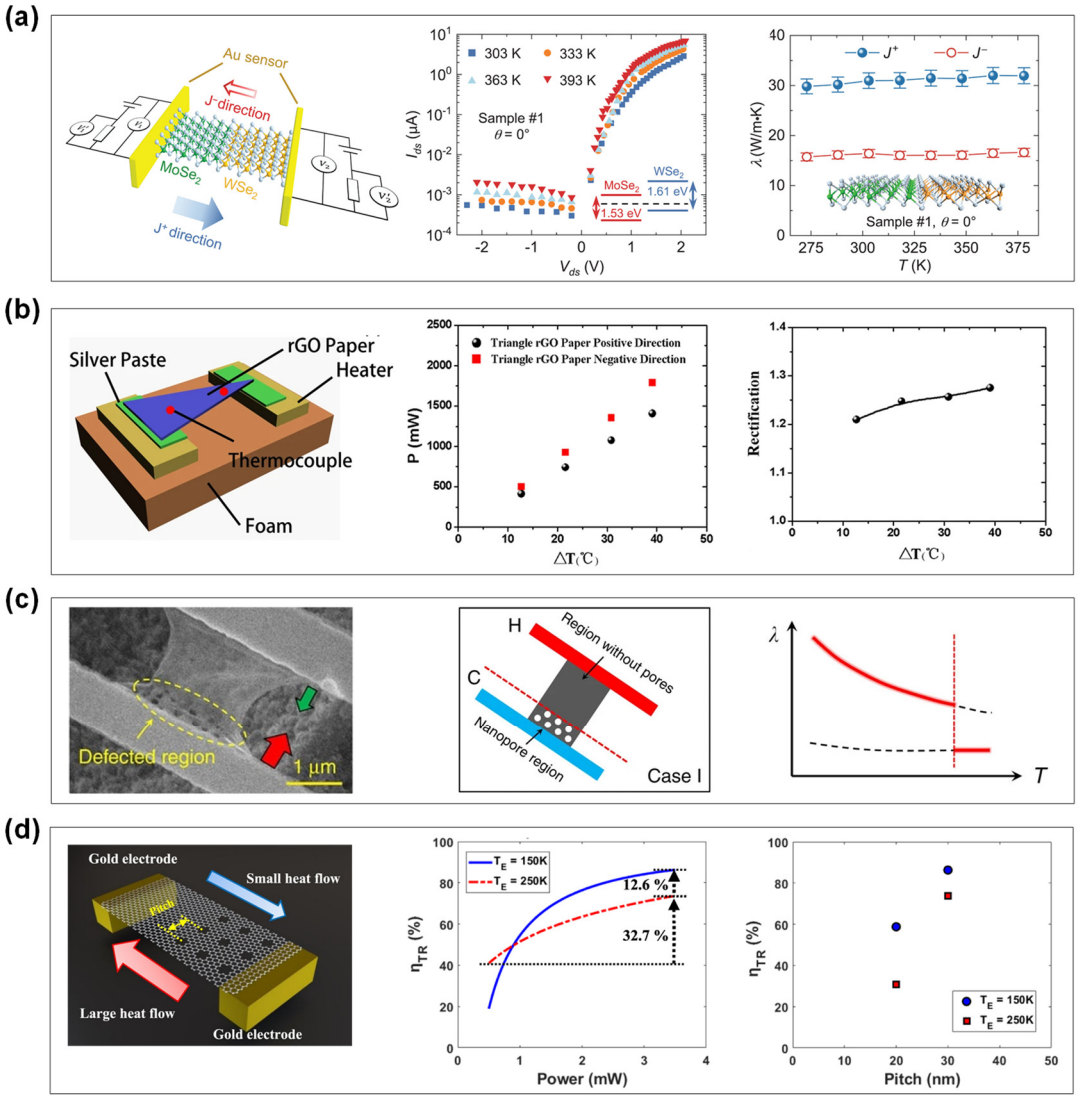

Figure 7. Thermal rectifiers based on 2D materials. (**a**) $MoSe_2$-WSe_2 lateral heterostructure measured by an H-type sensing device; the electrical and thermal transport data show a preferred high-conductance heat-flow direction from $MoSe_2$ to WSe_2 and a suppressed reverse direction. Copyright 2022, AAAS [30]. (**b**) Triangular rGO paper device on a heater and thermocouple, with measured heat power and thermal rectification coefficient as a function of the applied temperature difference ΔT. Copyright 2012, Springer Nature [29]. (**c**) Suspended graphene partially patterned with nanopores, where heat flows from the pristine region to the nanopore region, together with temperature-dependent thermal conductivity curves comparing graphene with and without nanopores. Copyright 2017, Springer Nature [32]. (**d**) Half-meshed suspended graphene device, showing asymmetric heat flow and the corresponding thermal rectification ratio as a function of input power and nanomesh pitch at different environmental temperatures. Copyright 2021 IOP Publishing [31].

Numerous simulations have predicted the feasibility of high rectification ratios in 2D materials, but the performance of actual devices is often limited by size and fabrication constraints. At the macroscopic scale, experimental attempts have been made; for example, Tian et al. fabricated triangular and double-rectangular thermal rectifiers from large-area reduced graphene oxide paper [29]. Under a temperature bias of about 12 K, this rGO thermal diode exhibited a maximal rectification ratio of about 1.21, meaning that the forward thermal conductance was 21% higher than the reverse conductance, as shown in Figure 7b. This result demonstrated that a substantial rectification effect can be achieved in a macroscopic device made of layered graphene-based material, and increasing structural asymmetry can further improve the rectification ratio. At the micro- and nanoscale, in 2017 Wang et al. reported the first experimental demonstration of a suspended monolayer graphene thermal rectifier. Using an H-type microbridge measurement method, they patterned a single graphene sheet with asymmetric defects and a tapered-width region. Two types of rectification behavior were measured: in one asymmetric sample containing nanopore defects, the thermal conductivity for heat flow from the perforated region to the pristine region was about 26% higher than in the opposite direction; in another sample with gradually narrowing width and one side decorated with nanoparticles, the thermal conductivity for heat flow from the wide and clean side to the narrow and decorated side was about 10% higher than in the opposite direction, as shown in Figure 7c [32]. Although these rectification ratios are lower than the multi-fold values predicted by simulations, they clearly demonstrate rectification in graphene at room temperature, and the experimental data are qualitatively consistent with molecular dynamics simulations. Liu et al. investigated graphene-based thermal rectification by measuring the thermal transport properties of asymmetric suspended graphene nanomesh devices [31]. They patterned a sub-10 nm periodic nanopore phononic crystal on half of a suspended graphene ribbon using helium ion beam milling, and developed a differential thermal leakage technique to extract thermal transport without interference from electronic leakage through the bridge. As shown in Figure 7d, in a typical device with a 20 nm nanopore pitch, they reported a thermal rectification ratio up to 60%. Within a certain range, increasing the nanopore pitch further enhanced the rectification ratio, whereas raising the environmental temperature degraded it. These results demonstrate that introducing phononic-crystal asymmetry into a homogeneous graphene sheet is an effective route toward high-performance thermal rectifiers. For heterojunction-based rectification, the above-mentioned $MoSe_2/WSe_2$ lateral heterojunction study achieved not only an electrical rectification ratio up to 10^4 but also nearly 100% thermal rectification. Moreover, by changing the orientation angle of the heterojunction interface, the rectification factor could be tuned from a maximum value to nearly zero. This work combined thermal rectification with electronic functionality and illustrated the potential of 2D heterojunctions in thermal management and energy applications.

Overall, 2D thermal rectifiers have progressed from simulation to experimental verification, with typical rectification ratios around 10–50%. Remaining challenges include maintaining high rectification ratios over a broad temperature range and at higher heat flux, and achieving device-level integration and stability. In experiments, some designs that enhance rectification often reduce overall conductance or mechanical robustness, and device-to-device reproducibility still needs improvement. Further advances in nanofabrication and heterogeneous integration, together with the development of tunable thermal rectification under external stimuli such as electric fields and mechanical stress, will be required to move 2D thermal diodes closer to practical applications.

4.2. Thermal Transistor

Building on thermal rectification, a thermal transistor introduces a third terminal to control heat flow and thereby enables switching and amplification of thermal signals. In 2006, Li et al. proposed a theoretical model of a thermal transistor: by connecting in series two thermal diodes that exhibit NDTR, the main heat flow can be amplified and modulated, as shown in Figure 8a [11]. Operation of such a device requires the material to show nonlinear thermal transport in a certain temperature range, so that a small temperature change at the control terminal induces a large change in heat flow at the output and an effective thermal amplification factor. For 2D materials, realizing NDTR and three-terminal control mainly relies on constructing complex heterostructures or systems with coupled functionalities. For example, one theoretical study proposed adding a control branch to a graphene Y-junction; when this control branch is heated, nonlinear phonon scattering can reduce the effective thermal conductance of another main channel, producing a heat-switching effect [131].

One representative scheme is to use electrochemical intercalation to alter phonon scattering in a 2D material. Sood et al. reported an electrochemical thermal transistor based on an MoS_2 film: by reversibly intercalating and de-intercalating lithium ions to modify the lattice structure of MoS_2, they achieved nearly an order-of-magnitude difference in thermal conductivity at room temperature between the on state (pristine MoS_2) and the off state

(Li_xMoS_2 after Li intercalation) [36]. TDTR microscopy measurements of the lithium distribution, together with first-principles calculations, showed that intercalation introduces a lithium rattling mode, c-axis strain and stacking disorder, all of which enhance phonon scattering and strongly reduce thermal conductivity. This device achieved a thermal on/off ratio of about 10, demonstrating reversible and controllable modulation of heat conduction at the nanoscale. Another design is an electrically driven mechanical thermal transistor, which uses an electric field to deform a 2D material and thus control thermal contact. Chen et al. demonstrated a graphene membrane thermal switch: by applying about 2 V between electrodes above and below a suspended graphene membrane, they caused it to collapse into contact with the substrate, thereby changing the thermal resistance under the membrane [132]. Scanning thermal microscopy showed that when graphene changes from the suspended state (off state) to the adhered state (on state), cross-membrane heat flow increases and the probe temperature drops significantly. The on/off thermal conductance ratio of this switch is about 1.3. Although this change is modest, the ultralow heat capacity and very fast mechanical response of the graphene membrane indicate that switching times on the order of nanoseconds may be achievable. More importantly, this design shows that the mechanical flexibility of 2D materials can be used to construct thermal conduction modulation elements in which the suspended and contacted configurations correspond to distinct thermal states without direct solid-solid electrical contact, thereby avoiding electrical leakage.

A thermal transistor is expected to provide a high thermal amplification factor and well-defined on and off states, but most 2D-material thermal transistor studies so far focus on switching-type modulation, namely reversible changes in thermal conductance, while continuous amplification and logic functionality remain at an early stage. Experimentally, the electrochemically intercalated MoS_2 thermal switch has achieved the largest conductance switching ratio to date, about 10, but its switching speed is limited by ion diffusion and lies on the order of minutes The graphene switch offers potentially sub-microsecond speeds, but the magnitude of its conductance change is limited to about 30%. Efficient thermal transistors face both material and structural challenges: materials must exhibit strong nonlinear thermal transport, and the device geometry must provide effective three-terminal coupling to achieve significant heat-flow amplification. Nonetheless, 2D materials provide several unique platforms for attempts to construct high-performance thermal transistors. With improvements in material quality and advances in nanomanufacturing, these platforms should make it possible to realize thermal transistor components with true amplification, forming a basis for thermal logic circuits.

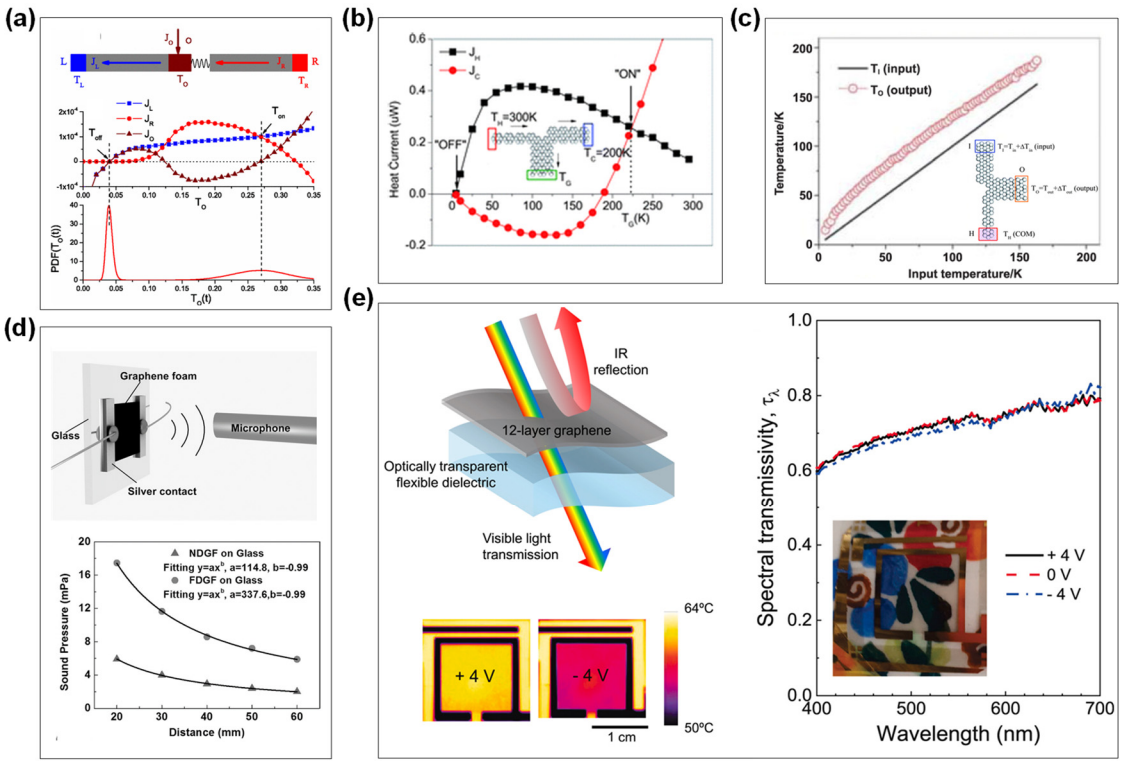

Figure 8. Thermal devices based on 2D materials: transistor, memory, and others. (**a**) Theoretical model of a thermal memory, showing heat currents versus control temperature and the probability distribution of the particle temperature. Copyright 2008, AIP Publishing [11]. (**b**) Three-terminal graphene nanoribbon acting as a thermal switch, where tuning the gate temperature switches the device between low-conductance (OFF) and high-

conductance (ON) states. (**c**) Graphene-based three-terminal structure operating as a thermal amplifier, in which a small change of input temperature produces an amplified change of output temperature with gain larger than one. Copyright 2011, Royal Society of Chemistry [133]. (**d**) Thermoacoustic loudspeaker using graphene foam as the sound-emitting element, together with measured sound pressure versus distance for different graphene foam configurations. Copyright 2015, Wiley-VCH [34]. (**e**) Graphene-based infrared camouflage device that is transparent in the visible range but allows active tuning of infrared emissivity via a multilayer graphene electrode, as demonstrated by thermal images and spectral transmissivity curves. Copyright 2019, Elsevier [134].

4.3. Thermal Memory

A thermal memory is a device that stores binary information in thermal states and exploits the ability of a system to retain a particular thermal condition. Constructing a thermal memory cell requires that the system have at least two thermal conductance or temperature states that can be stably maintained under the same external conditions, and that it can be reversibly switched between these states by an external thermal pulse. This typically requires that the material or structure exhibit hysteresis in heat transport; that is, the thermal conductance follows different paths during heating and cooling so that two stable thermal conductance or temperature states exist and can represent the logical values 0 and 1. In 2008, Wang and Li proposed the first thermal memory model: by connecting two thermal diodes in series to form a feedback loop and introducing nonlinear thermal conductance, the system can attain two stable temperature solutions and thereby store thermal information.[13] This concept, validated by numerical simulation, showed that nonlinear device elements such as thermal diodes and NDTR materials are essential building blocks for thermal memory, as shown in Figure 8b,c.

Phase-change materials, whose thermal conductivity shows both strong temperature dependence and hysteresis, are regarded as promising candidates for implementing solid-state thermal memory.[135,136] For example, single-crystalline VO_2 undergoes a metal-insulator transition at about 68 °C with abrupt changes in lattice structure and carrier concentration, which causes its thermal conductivity to follow different trajectories during heating and cooling. Xie et al. constructed a VO_2 nanobeam thermal memory device [35]. A VO_2 nanobeam was connected between the thermal input and output terminals. When the input temperature T_{in} rose above the VO_2 phase transition regime, the nanobeam switched from the insulating to the metallic state and its heat-carrying ability increased markedly; upon cooling, the return to the insulating state was delayed by about 4–5 K, so that after T_{in} fell below the transition region, the material remained in the high-conductivity metallic phase over a finite temperature range. This hysteresis caused the output terminal temperature T_{out} to follow different branches during heating and cooling, with the high-conductivity branch corresponding to one logical state and the low-conductivity branch to the other. Experiments showed that under purely thermal excitation, without external electrical bias, the output temperature difference relative to the input adopted one of two stable values, and the difference between these values could be amplified by nearly two orders of magnitude. Thus, a small change in input temperature can produce a large and readable output signal, which corresponds to thermal write and read operations. Measurements of the nanobeam resistance as a function of temperature further indicated that the hysteresis in VO_2 thermal conductivity is dominated by the electronic contribution to thermal conductance.

Using thermal conductivity hysteresis induced by molecular configuration changes provides another route to thermal memory. Zhao et al. fabricated a polymer nanofiber containing double hydrogen bonds, forming a hydrogen-bonded network based on melamine-quinazoline molecules [137]. This material exhibited two clear thermal conductivity hysteresis loops around about 297 K and 317 K, with a maximum thermal conductivity difference of 66.7% between the two states. On this basis, they designed a fully solid-state thermal memory device: multiple polymer nanofibers were connected between a suspended heater island and a sensor island, and by periodically driving the heater temperature they achieved repeated reversible write and erase operations near room temperature. When the heater temperature rose above a high threshold, some hydrogen bonds in the fibers broke and the material entered a low-κ state; upon cooling below the threshold, the hydrogen bonds reformed but with a lag relative to the temperature change, so that the material remained in a different thermal conductance state corresponding to a high-κ branch. Through multiple cycles, this polymer thermal memory showed stable and repeatable switching and was able to use phonon transport states directly to store information at room temperature. This was the first experimental demonstration that tuning intermolecular weak bonds can produce hysteretic modulation of purely phononic heat conduction.

Existing thermal memory devices still have relatively limited data retention. For example, an early simulation based on carbon nanomaterials estimated a storage lifetime on the order of 100 microseconds. Connecting multiple devices in parallel can extend the effective hold time, but there is still a large gap compared with electronic memory. Environmental thermal radiation and random temperature fluctuations can further compromise the

stability of phononic storage. A thermal memory that relies entirely on 2D materials has not yet been demonstrated experimentally, but 2D materials already play important roles in interface engineering and signal readout. Integrating a VO_2 or polymer thermal memory cell with a graphene or MoS_2 transistor allows the thermal state to be read out electrically by exploiting the high electrical sensitivity of the 2D channel, forming a hybrid thermal-electrical memory unit. In addition, by creating local strain fields or ordered defect arrays in 2D materials, it is theoretically possible to obtain multistable heat-flow distributions in a purely phononic system. Thermal memory adds a temporal dimension to thermal logic, but there is still considerable scope for improving retention time, noise immunity and integrability.

4.4. Other Thermal Devices

Thermoacoustic speakers: Graphene's high electrical conductivity and very low heat capacity make it an efficient material for thermoacoustic conversion. When an alternating current passes through a graphene film, periodic heating and cooling cause the surrounding air to expand and contract thermally, generating sound pressure and thus an acoustic output [138]. This thermoacoustic effect does not require mechanical vibrating components and therefore offers simple structure and all-solid-state implementation, as shown in Figure 8d [34]. Challenges for this type of device include improving acoustic efficiency, which is still relatively low compared to conventional electromagnetic speakers, and managing heat dissipation, but the planar and miniature form factor makes them promising for ultrathin loudspeakers and wearable audio devices.

Thermal camouflage and infrared modulation: Infrared thermal cloaking devices aim to control an object's thermal radiation so that it blends with the environment and avoids infrared detection. The infrared emissivity of graphene can be dynamically tuned by electrostatic gating, offering a route to active thermal camouflage [139]. A recent study constructed a flexible transparent graphene thermal camouflage film: an ionic-liquid gate and a multilayer graphene stack were integrated on a PET substrate, and an applied gate voltage changed the carrier density in graphene and thus its infrared emissivity, as shown in Figure 8e [134]. Experiments achieved modulation of emissivity in the 3–5 μm band from about 0.9 down to about 0.3 without affecting visible transparency, and showed that the device can adjust infrared emission against different backgrounds to mimic the ambient temperature, effectively concealing the object. Besides tuning emissivity, the high thermal conductivity of graphene can be used to redistribute surface temperature: coating a surface with a graphene film can rapidly spread local hot spots so that external infrared imaging finds it difficult to locate the true internal heat source [140]. For general infrared modulation, such as smart thermal camouflage textiles or tunable infrared beacons, graphene devices offer low-power and fast-response solutions, although achieving large-area uniform coatings, high modulation depth and long-term durability remains challenging.

Thermal sensing and detection: The combination of graphene with other functional materials has led to significant advances in thermal sensing. Sassi et al. combined a monolayer graphene field-effect transistor with a pyroelectric $LiNbO_3$ crystal to construct an ultra-sensitive mid-infrared detector [33]. When $LiNbO_3$ is heated by incident infrared radiation and produces surface charge, a suspended top gate couples this charge to the graphene channel and modulates its resistance, thereby amplifying the electrical signal associated with a small temperature rise. An equivalent temperature coefficient of resistance as high as 900% K^{-1} was achieved, much higher than the 2–4% K^{-1} typical of conventional materials, enabling detection of temperature changes as small as 15 μK. Graphene's low noise and nearly linear response are crucial in allowing the pyroelectric signal to be read with high gain. Graphene-based thermal sensors feature fast response, small size and easy integration, and are promising for infrared imaging, environmental monitoring and biomedical applications. In such composite devices, graphene usually acts as the signal transduction layer rather than the main medium for heat storage or transport, but its presence improves the performance of traditional thermal sensing technologies.

Other novel devices: 2D materials have also been explored for use in thermal logic gates, electrothermal-optical hybrid devices and other functions. For example, combining a graphene thermal rectifier with a thermal transistor can realize basic AND and OR thermal logic functions [12]. Anisotropic 2D materials such as black phosphorus can be used to design thermal isolation and guiding structures that act as thermal waveguides or thermal lenses for localized chip cooling. Phononic crystal structures have also been proposed: by introducing periodic nanopore arrays into 2D materials to control the propagation of phonons in selected frequency ranges, frequency-selective control of thermal conductivity can be achieved [141]. These concepts are mostly at the theoretical or proof-of-concept stage, but they indicate the potential of 2D materials for multifunctional integration in thermal devices.

In summary, the emergence of 2D materials has provided a versatile platform for thermal devices. One-way heat-flow thermal diodes, thermal switches and transistors with tunable conductance, thermal memories that retain

thermal histories and thermoacoustic or infrared modulation devices across different scales have all seen substantial progress. At the same time, most of these devices are still at the proof-of-concept and performance-optimization stage, and fully integrated thermal circuits have not yet been realized. Further development will require close interaction between experiment and theory, continual refinement of device designs, introduction of new materials and structures and solutions to engineering challenges such as device uniformity and large-scale integration.

5. Summary and Outlook

This review has traced the development of thermal research in 2D materials, focusing on phonon engineering approaches and the theoretical and experimental progress of various thermal functional devices. Overall, with the advent of 2D materials such as graphene, researchers have been able to manipulate phonon spectra and transport in atomically thin crystals, realizing functionalities such as thermal rectification, thermal switching and thermal memory that are not attainable in traditional 3D materials. Early studies were predominantly based on theoretical simulations and showed that asymmetric geometry, interfacial scattering, external field control and related strategies can generate a range of nontrivial heat transport phenomena in 2D materials. A series of experiments gradually validated concepts such as graphene thermal diodes, suspended-membrane thermal switches, MoS_2 thermal transistors and VO_2 thermal memory devices. These advances indicate that phononics is moving from purely theoretical proposals toward experimental reality, with 2D materials acting as key platform materials. At the same time, most 2D thermal devices are still at the single-device demonstration stage. Compared with electronic devices, their performance and scalability remain limited: rectifiers and thermoelectric devices already have some experimental basis, but thermal transistors and thermal logic gates largely remain at the theoretical or early experimental stage without system-level validation. Graphene has been studied most extensively, whereas the thermal potential of other 2D materials, such as black phosphorus and anisotropic transition-metal chalcogenides, has not yet been fully explored.

Several directions are particularly important for the further development of 2D thermal research and applications:

(1) Deeper understanding of phonon transport mechanisms. Although phonon behavior at the nanoscale can be simulated using molecular dynamics, phonon Boltzmann transport equations and related tools, many fundamental aspects of phonon transport are still less well understood than electronic transport. In-depth studies of phonon turbulence, second sound, which can be viewed as quantized heat waves, and other non-classical transport phenomena will be valuable for designing materials with ultra-low or ultra-high thermal conductivity [142]. Equally important is control of interfacial phonon states. Because 2D materials are often used in heterojunctions, a more refined understanding of how phonons propagate in 2D materials and across their interfaces will enable more effective design and optimization of thermal devices.

(2) Thermal device structure design and multifunctional integration. Current 2D thermal device research mostly focuses on single-function proof-of-concept demonstrations, and complex integrated thermal circuits have not yet been realized. An important direction is to pursue innovative material and structural designs that enable multifunctional devices with coupled electrical, thermal and optical responses. 2D materials provide advantages for these tasks: their ultrathin nature allows vertical stacking to build 3D thermal circuits, and their strong anisotropy can be used to pattern conductive pathways that guide heat flow. Realizing such integration requires overcoming compatibility and interference between different physical fields; for instance, the temperature rise of an operating thermal device can affect the performance of nearby electronic components and must be mitigated through material choices, such as heat-tolerant 2D semiconductors, and through structural isolation. Addressing these issues will require high-precision nanofabrication and transfer techniques, as well as standardized methods for characterizing thermal device performance, which are essential for large-scale integration.

(3) Application of artificial intelligence (AI). As data from 2D materials and nanoscale phononics accumulate, introducing AL and machine learning (ML) can accelerate materials discovery and device optimization. On the materials side, machine-learning models can be used for phonon property prediction and material screening. By training on existing first-principles datasets, a model can rapidly predict the phonon dispersion and thermal conductivity of a given 2D material or heterostructure, and thereby identify candidates with high rectification efficiency or specific phonon modes [143–145]. In the future, a dedicated 2D materials phonon database could be established, and AI methods could be used to mine relationships between composition, structure and thermal performance in order to guide experimental synthesis. AI is likely to become an effective tool in thermal science research, helping to identify optimization strategies in the large parameter space of materials and structures.

In summary, the thermal science of 2D materials is at a transition point between basic research and practical application. Further progress requires a deeper understanding of fundamental phonon transport in order to overcome current performance bottlenecks. It is also necessary to address device-level integration and reliability

issues that arise in realistic operating conditions, and to broaden the application prospects of 2D thermal devices in thermal management, energy conversion and unconventional computing. With the combined development of materials science, nanotechnology and artificial intelligence, phononic devices are expected to move from laboratory demonstrations to practical applications. The ability to precisely control heat, traditionally regarded mainly as a by-product of electronic operation, may thus become a new type of information carrier in future technologies.

Author Contributions

J.L.: methodology, formal analysis, data curation, writing—original draft. S.C.: visualization, investigation, formal analysis. H.W.: writing—review & editing, funding acquisition. All authors have read and agreed to the published version of the manuscript.

Funding

This work was supported by the National Natural Science Foundation of China (No. 52172046).

Conflicts of Interest

The authors declare no conflict of interest.

Use of AI and AI-Assisted Technologies

No AI tools were utilized for this paper.

References

1. Mori, N.; Ando, T. Electron optical-phonon interaction in single and double heterostructures. *Phys. Rev. B* **1989**, *40*, 6175–6188. https://doi.org/10.1103/PhysRevB.40.6175.
2. Regner, K.T.; Sellan, D.P.; Su, Z.H.; et al. Broadband phonon mean free path contributions to thermal conductivity measured using frequency domain thermoreflectance. *Nat. Commun.* **2013**, *4*, 1640. https://doi.org/10.1038/ncomms2630.
3. Peierls, R. The kinetic theory of thermal conduction in crystals. *Ann. Phys.* **1929**, *3*, 1055–1101.
4. Slack, G.A. Nonmetallic crystals with high thermal-conductivity. *J. Phys. Chem. Solids* **1973**, *34*, 321–335. https://doi.org/10.1016/0022-3697(73)90092-9.
5. Chen, H.; Zhang, W.; Niu, Q.; et al. Chiral phonons in two-dimensional materials. *2D Mater.* **2019**, *6*, 012002. https://doi.org/10.1088/2053-1583/aaf292.
6. Zhao, Y.Y.; Wang, J.H.; Gao, W.W.; et al. Topological and chiral phonons in two-dimensional transitional metal monocarbide monolayers. *Appl. Phys. Lett.* **2026**, *128*, 072203. https://doi.org/10.1063/5.0302582.
7. Li, N.B.; Ren, J.; Wang, L.; et al. Colloquium: Phononics: Manipulating heat flow with electronic analogs and beyond. *Rev. Mod. Phys.* **2012**, *84*, 1045–1066. https://doi.org/10.1103/RevModPhys.84.1045.
8. Xie, S.Q.; Zhu, H.X.; Zhang, X.; et al. A brief review on the recent development of phonon engineering and manipulation at nanoscales. *Int. J. Extrem. Manuf.* **2024**, *6*, 012007. https://doi.org/10.1088/2631-7990/acfd68.
9. Terraneo, M.; Peyrard, M.; Casati, G. Controlling the energy flow in nonlinear lattices: A model for a thermal rectifier. *Phys. Rev. Lett.* **2002**, *88*, 094302. https://doi.org/10.1103/PhysRevLett.88.094302.
10. Li, B.W.; Wang, L.; Casati, G. Thermal diode: Rectification of heat flux. *Phys. Rev. Lett.* **2004**, *93*, 184301. https://doi.org/10.1103/PhysRevLett.93.184301.
11. Li, B.W.; Wang, L.; Casati, G. Negative differential thermal resistance and thermal transistor. *Appl. Phys. Lett.* **2006**, *88*, 143501. https://doi.org/10.1063/1.2191730.
12. Wang, L.; Li, B. Thermal logic gates: Computation with phonons. *Phys. Rev. Lett.* **2007**, *99*, 177208. https://doi.org/10.1103/PhysRevLett.99.177208.
13. Wang, L.; Li, B.W. Thermal memory: A storage of phononic information. *Phys. Rev. Lett.* **2008**, *101*, 267203. https://doi.org/10.1103/PhysRevLett.101.267203.
14. Rurali, R. A one-way street for phonon transport: Past, present and future of solid-state thermal rectification. *Nano Express* **2024**, *5*, 011001. https://doi.org/10.1088/2632-959X/ad2a17.
15. Pop, E. Energy dissipation and transport in nanoscale devices. *Nano Res.* **2010**, *3*, 147–169. https://doi.org/10.1007/s12274-010-1019-z.
16. Wang, Y.X.; Xu, N.; Li, D.Y.; et al. Thermal properties of two dimensional layered materials. *Adv. Funct. Mater.* **2017**, *27*, 1604134. https://doi.org/10.1002/adfm.201604134.
17. Wang, L.; Li, B. Phononics gets hot. *Phys. World* **2008**, *21*, 27–29.
18. Xu, S.; Xu, Y.R.; Zhang, J.C.; et al. Ballistic transport enhanced heat convection at nanoscale hotspots. *J. Appl. Phys.*

2024, *136*, 164306. https://doi.org/10.1063/5.0221352.
19. Song, H.F.; Liu, J.M.; Liu, B.L.; et al. Two-dimensional materials for thermal management applications. *Joule* **2018**, *2*, 442–463. https://doi.org/10.1016/j.joule.2018.01.006.
20. Balandin, A.A. Thermal properties of graphene and nanostructured carbon materials. *Nat. Mater.* **2011**, *10*, 569–581. https://doi.org/10.1038/nmat3064.
21. Liu, B.L.; Köpf, M.; Abbas, A.N.; et al. Black arsenic-phosphorus: Layered anisotropic infrared semiconductors with highly tunable compositions and properties. *Adv. Mater.* **2015**, *27*, 4423–4429. https://doi.org/10.1002/adma.201501758.
22. Novoselov, K.S.; Geim, A.K.; Morozov, S.V.; et al. Electric field effect in atomically thin carbon films. *Science* **2004**, *306*, 666–669. https://doi.org/10.1126/science.1102896.
23. Golberg, D.; Bando, Y.; Huang, Y.; et al. Boron nitride nanotubes and nanosheets. *ACS Nano* **2010**, *4*, 2979–2993. https://doi.org/10.1021/nn1006495.
24. Zhang, Y.F.; Han, D.; Zhao, Y.H.; et al. High-performance thermal interface materials consisting of vertically aligned graphene film and polymer. *Carbon* **2016**, *109*, 552–557. https://doi.org/10.1016/j.carbon.2016.08.051.
25. Liu, L.Q.; Xu, C.C.; Yang, Y.Q.; et al. Graphene-based polymer composites in thermal management: Materials, structures and applications. *Mater. Horiz.* **2025**, *12*, 64–91. https://doi.org/10.1039/d4mh00846d.
26. Tabor, P.; Ignuta-Ciuncanu, M.C.; Martinez-Botas, R.F. Thermal diodes, transistors and logic: Review of unconventional computing methods. *Biosystems* **2025**, *254*, 105491. https://doi.org/10.1016/j.biosystems.2025.105491.
27. Renteria, J.D.; Nika, D.L.; Balandin, A.A. Graphene thermal properties: Applications in thermal management and energy storage. *Appl. Sci.* **2014**, *4*, 525–547. https://doi.org/10.3390/app4040525.
28. Yan, Z.; Nika, D.L.; Balandin, A.A. Thermal properties of graphene and few-layer graphene: Applications in electronics. *IET Circuits Devices Syst.* **2015**, *9*, 4–12. https://doi.org/10.1049/iet-cds.2014.0093.
29. Tian, H.; Xie, D.; Yang, Y.; et al. A novel solid-state thermal rectifier based on reduced graphene oxide. *Sci. Rep.* **2012**, *2*, 523. https://doi.org/10.1038/srep00523.
30. Zhang, Y.; Lv, Q.; Wang, H.; et al. Simultaneous electrical and thermal rectification in a monolayer lateral heterojunction. *Science* **2022**, *378*, 169–175. https://doi.org/10.1126/science.abq0883.
31. Liu, F.Y.L.; Muruganathan, M.; Feng, Y. Thermal rectification on asymmetric suspended graphene nanomesh devices. *Nano Futures* **2021**, *5*, 045002. https://doi.org/10.1088/2399-1984/ac36b5.
32. Wang, H.D.; Hu, S.Q.; Takahashi, K.; et al. Experimental study of thermal rectification in suspended monolayer graphene. *Nat. Commun.* **2017**, *8*, 15843. https://doi.org/10.1038/ncomms15843.
33. Sassi, U.; Parret, R.; Nanot, S.; et al. Graphene-based mid-infrared room-temperature pyroelectric bolometers with ultrahigh temperature coefficient of resistance. *Nat. Commun.* **2017**, *8*, 14311. https://doi.org/10.1038/ncomms14311.
34. Fei, W.W.; Zhou, J.X.; Guo, W.L. Low-voltage driven graphene foam thermoacoustic speaker. *Small* **2015**, *11*, 2252–2256. https://doi.org/10.1002/smll.201402982.
35. Xie, R.G.; Bui, C.T.; Varghese, B.; et al. An electrically tuned solid-state thermal memory based on metal-insulator transition of single-crystalline VO_2 nanobeams. *Adv. Funct. Mater.* **2011**, *21*, 1602–1607. https://doi.org/10.1002/adfm.201002436.
36. Sood, A.; Xiong, F.; Chen, S.D.; et al. An electrochemical thermal transistor. *Nat. Commun.* **2018**, *9*, 4510. https://doi.org/10.1038/s41467-018-06760-7.
37. Yigen, S.; Champagne, A.R. Wiedemann-Franz relation and thermal-transistor effect in suspended graphene. *Nano Lett.* **2014**, *14*, 289–293. https://doi.org/10.1021/nl403967z.
38. Qian, X.; Zhou, J.; Chen, G. Phonon-engineered extreme thermal conductivity materials. *Nat. Mater.* **2021**, *20*, 1188–1202. https://doi.org/10.1038/s41563-021-00918-3.
39. Lindsay, L.; Broido, D.A.; Mingo, N. Flexural phonons and thermal transport in graphene. *Phys. Rev. B* **2010**, *82*, 6115427. https://doi.org/10.1103/PhysRevB.82.115427.
40. Feng, T.L.; Ruan, X.L. Four-phonon scattering reduces intrinsic thermal conductivity of graphene and the contributions from flexural phonons. *Phys. Rev. B* **2018**, *97*, 045202. https://doi.org/10.1103/PhysRevB.97.045202.
41. Dai, W.; Wang, Y.D.; Li, M.H.; et al. 2D materials-based thermal interface materials: Structure, properties, and applications. *Adv. Mater.* **2024**, *36*, e2311335. https://doi.org/10.1002/adma.202311335.
42. Fu, Y.F.; Hansson, J.; Liu, Y.; et al. Graphene related materials for thermal management. *2D Mater.* **2020**, *7*, 012001. https://doi.org/10.1088/2053-1583/ab48d9.
43. Radisavljevic, B.; Radenovic, A.; Brivio, J.; et al. Single-layer MoS_2 transistors. *Nat. Nanotechnol.* **2011**, *6*, 147–150. https://doi.org/10.1038/nnano.2010.279.
44. Balandin, A.A.; Ghosh, S.; Bao, W.Z.; et al. Superior thermal conductivity of single-layer graphene. *Nano Lett.* **2008**, *8*, 902–907. https://doi.org/10.1021/nl0731872.
45. Zhou, H.Q.; Zhu, J.X.; Liu, Z.; et al. High thermal conductivity of suspended few-layer hexagonal boron nitride sheets. *Nano Res.* **2014**, *7*, 1232–1240. https://doi.org/10.1007/s12274-014-0486-z.
46. Hu, Y.X.; Li, D.; Feng, C.B.; et al. Nanostructure engineering of two-dimensional diamonds toward high thermal

conductivity and approaching zero Poisson's ratio. *PCCP* **2022**, *24*, 15340–15348. https://doi.org/10.1039/d2cp01745h.

47. Fan, H.; Wu, H.; Lindsay, L.; et al. Ab initio investigation of single-layer high thermal conductivity boron compounds. *Phys. Rev. B* **2019**, *100*, 085420. https://doi.org/10.1103/PhysRevB.100.085420.
48. Yan, R.S.; Simpson, J.R.; Bertolazzi, S.; et al. Thermal conductivity of monolayer molybdenum disulfide obtained from temperature-dependent raman spectroscopy. *ACS Nano* **2014**, *8*, 986–993. https://doi.org/10.1021/nn405826k.
49. Luo, Z.; Maassen, J.; Deng, Y.X.; et al. Anisotropic in-plane thermal conductivity observed in few-layer black phosphorus. *Nat. Commun.* **2015**, *6*, 8572. https://doi.org/10.1038/ncomms9572.
50. Pettes, M.T.; Maassen, J.; Jo, I.; et al. Effects of surface band bending and scattering on thermoelectric transport in suspended bismuth telluride nanoplates. *Nano Lett.* **2013**, *13*, 5316–5322. https://doi.org/10.1021/nl402828s.
51. Li, J.W.; Zheng, J.; Yang, Y.J.; et al. Thickness-dependent low lattice thermal conductivity of chemical vapor-deposited $SnSe_2$ nanosheets. *ACS Nano* **2025**, *19*, 33324–33334. https://doi.org/10.1021/acsnano.5c09332.
52. Ran, Y.T.; Meng, C.; Ma, Y.P.; et al. Reduced thermal conductivity in $SnSe_2$ moire superlattices. *ACS Nano* **2025**, *19*, 10452–10460. https://doi.org/10.1021/acsnano.5c00295.
53. Zhao, S.Y.; Wang, H.W. An integrated H-type method to measure thermoelectric properties of two-dimensional materials. *ES Energy Environ.* **2020**, *9*, 59–66. https://doi.org/10.30919/esee8c262.
54. Oh, D.W.; Jain, A.; Eaton, J.K.; et al. Thermal conductivity measurement and sedimentation detection of aluminum oxide nanofluids by using the 3ω method. *Int. J. Heat. Fluid. Flow.* **2008**, *29*, 1456–1461. https://doi.org/10.1016/j.ijheatfluidflow.2008.04.007.
55. Heron, J.S.; Fournier, T.; Mingo, N.; et al. Mesoscopic size effects on the thermal conductance of silicon nanowire. *Nano Lett.* **2009**, *9*, 1861–1865. https://doi.org/10.1021/nl803844j.
56. Li, Q.Y.; Zhang, X.; Hu, Y.D. Laser flash Raman spectroscopy method for thermophysical characterization of 2D nanomaterials. *Thermochim. Acta* **2014**, *592*, 67–72. https://doi.org/10.1016/j.tca.2014.08.011.
57. Zobeiri, H.; Hunter, N.; Xu, S.; et al. Robust and high-sensitivity thermal probing at the nanoscale based on resonance Raman ratio (R3). *Int. J. Extrem. Manuf.* **2022**, *4*, 035201. https://doi.org/10.1088/2631-7990/ac6cb1.
58. Verma, P. Tip-enhanced Raman spectroscopy: Technique and recent advances. *Chem. Rev.* **2017**, *117*, 6447–6466. https://doi.org/10.1021/acs.chemrev.6b00821.
59. Huang, D.Z.; Sun, Q.S.; Liu, Z.Y.; et al. Ballistic thermal transport at sub-10 nm laser-induced hot spots in GaN crystal. *Adv. Sci.* **2023**, *10*, e2204777. https://doi.org/10.1002/advs.202204777.
60. Jiang, P.Q.; Qian, X.; Yang, R.G. Time-domain thermoreflectance (TDTR) measurements of anisotropic thermal conductivity using a variable spot size approach. *Rev. Sci. Instrum.* **2017**, *88*, 074901. https://doi.org/10.1063/1.4991715.
61. Xu, S.; Fan, A.R.; Wang, H.D.; et al. Raman-based nanoscale thermal transport characterization: A critical review. *Int. J. Heat. Mass. Transf.* **2020**, *154*, 119751. https://doi.org/10.1016/j.ijheatmasstransfer.2020.119751.
62. Zhang, H.J.; Lee, G.; Cho, K. Thermal transport in graphene and effects of vacancy defects. *Phys. Rev. B* **2011**, *84*, 115460. https://doi.org/10.1103/PhysRevB.84.115460.
63. Kazemian, S.; Fanchini, G. Electron-phonon interaction and lattice thermal conductivity from metals to 2D Dirac crystals: A review. *J. Phys. Condens. Matter* **2025**. https://doi.org/10.1088/1361-648X/ae1fca.
64. Al Taleb, A.; Wan, W.; Benedek, G.; et al. Electron-phonon coupling and phonon dynamics in single-layer $NbSe_2$ on graphene: The role of moire phonons. *ACS Nano* **2025**, *19*, 8895–8903. https://doi.org/10.1021/acsnano.4c16399.
65. Bai, Z.; He, D.; Fu, S.; et al. Recent progress in electron-phonon interaction of two-dimensional materials. *Nano Sel.* **2022**, *3*, 1112–1122. https://doi.org/10.1002/nano.202100367.
66. Jo, I.; Pettes, M.T.; Kim, J.; et al. Thermal conductivity and phonon transport in suspended few-layer hexagonal boron nitride. *Nano Lett.* **2013**, *13*, 550–554. https://doi.org/10.1021/nl304060g.
67. Koh, Y.K.; Bae, M.H.; Cahill, D.G.; et al. Heat conduction across monolayer and few-layer graphenes. *Nano Lett.* **2010**, *10*, 4363–4368. https://doi.org/10.1021/nl101790k.
68. Nika, D.L.; Askerov, A.S.; Balandin, A.A. Anomalous size dependence of the thermal conductivity of graphene ribbons. *Nano Lett.* **2012**, *12*, 3238–3244. https://doi.org/10.1021/nl301230g.
69. Zhao, W.W.; Wang, Y.L.; Wu, Z.T.; et al. Defect-engineered heat transport in graphene: A route to high efficient thermal rectification. *Sci. Rep.* **2015**, *5*, 11962. https://doi.org/10.1038/srep11962.
70. Bonini, N.; Garg, J.; Marzari, N. Acoustic phonon lifetimes and thermal transport in free-standing and strained graphene. *Nano Lett.* **2012**, *12*, 2673–2678. https://doi.org/10.1021/nl202694m.
71. Zhang, Y.F.; Lv, Q.; Fan, A.R.; et al. Reduction in thermal conductivity of monolayer WS_2 caused by substrate effect. *Nano Res.* **2022**, *15*, 9578–9587. https://doi.org/10.1007/s12274-022-4560-7.
72. Lindsay, L.; Li, W.; Carrete, J.; et al. Phonon thermal transport in strained and unstrained graphene from first principles. *Phys. Rev. B* **2014**, *89*, 155426. https://doi.org/10.1103/PhysRevB.89.155426.
73. Duan, F.Q.; Wei, D.H.; Chen, A.L.; et al. Efficient modulation of thermal transport in two-dimensional materials for thermal management in device applications. *Nanoscale* **2023**, *15*, 1459–1483. https://doi.org/10.1039/d2nr06413h.

74. Chen, J.; Zhang, G.; Li, B.W. Substrate coupling suppresses size dependence of thermal conductivity in supported graphene. *Nanoscale* **2013**, *5*, 532–536. https://doi.org/10.1039/c2nr32949b.
75. Zhang, Z.W.; Hu, S.Q.; Chen, J.; et al. Hexagonal boron nitride: A promising substrate for graphene with high heat dissipation. *Nanotechnology* **2017**, *28*, 225704. https://doi.org/10.1088/1361-6528/aa6e49.
76. Li, T.; Tang, Z.N.; Huang, Z.X.; et al. Substrate effects on the thermal performance of in-plane graphene/hexagonal boron nitride heterostructures. *Carbon* **2018**, *130*, 396–400. https://doi.org/10.1016/j.carbon.2018.01.017.
77. Chen, X.K.; Hu, X.Y.; Jia, P.; et al. Tunable anisotropic thermal transport in porous carbon foams: The role of phonon coupling. *Int. J. Mech. Sci.* **2021**, *206*, 106576. https://doi.org/10.1016/j.ijmecsci.2021.106576.
78. Zhang, L.F.; Wang, J.S.; Li, B.W. Ballistic thermal rectification in nanoscale three-terminal junctions. *Phys. Rev. B* **2010**, *81*, 100301. https://doi.org/10.1103/PhysRevB.81.100301.
79. Hu, J.N.; Ruan, X.L.; Chen, Y.P. Molecular dynamics study of thermal rectification in graphene nanoribbons. *Int. J. Thermophys.* **2012**, *33*, 986–991. https://doi.org/10.1007/s10765-012-1216-y.
80. Yang, N.; Zhang, G.; Li, B.W. Thermal rectification in asymmetric graphene ribbons. *Appl. Phys. Lett.* **2009**, *95*, 033107. https://doi.org/10.1063/1.3183587.
81. Yousefi, F.; Shavikloo, M.; Mohammadi, M. Non-equilibrium molecular dynamics study on radial thermal conductivity and thermal rectification of graphene. *Mol. Simul.* **2019**, *45*, 646–651. https://doi.org/10.1080/08927022.2019.1578354.
82. Hu, J.N.; Ruan, X.L.; Chen, Y.P. Thermal conductivity and thermal rectification in graphene nanoribbons: A molecular dynamics study. *Nano Lett.* **2009**, *9*, 2730–2735. https://doi.org/10.1021/nl901231s.
83. Zhang, G.; Zhang, H.S. Thermal conduction and rectification in few-layer graphene Y Junctions. *Nanoscale* **2011**, *3*, 4604–4607. https://doi.org/10.1039/c1nr10945f.
84. Cheh, J.; Zhao, H. Thermal rectification in asymmetric U-shaped graphene flakes. *J. Stat. Mech.-Theory Exp.* **2012**, *2012*, 06011. https://doi.org/10.1088/1742-5468/2012/06/p06011.
85. Chen, X.K.; Liu, J.; Xie, Z.X.; et al. A local resonance mechanism for thermal rectification in pristine/branched graphene nanoribbon junctions. *Appl. Phys. Lett.* **2018**, *113*, 121906. https://doi.org/10.1063/1.5053233.
86. Xiao, P.; El Sachat, A.; Angel, E.C.; et al. MoS_2 phononic crystals for advanced thermal management. *Sci. Adv.* **2024**, *10*, eadm8825. https://doi.org/10.1126/sciadv.adm8825.
87. Wei, N.; Li, S.C.; Zhang, Y.Y.; et al. Thermal rectification of graphene on substrates with inhomogeneous stiffness. *Carbon.* **2019**, *154*, 81–89. https://doi.org/10.1016/j.carbon.2019.07.088.
88. Yang, X.; Zheng, X.H.; Liu, Q.S.; et al. Experimental study on thermal conductivity and rectification in suspended monolayer MoS_2. *ACS Appl. Mater. Interfaces* **2020**, *12*, 28306–28312. https://doi.org/10.1021/acsami.0c07544.
89. Wei, A.R.; Lahkar, S.; Li, X.X.; et al. Multilayer graphene-based thermal rectifier with interlayer gradient functionalization. *ACS Appl. Mater. Interfaces* **2019**, *11*, 45180–45188. https://doi.org/10.1021/acsami.9b11762.
90. Li, D.; Gong, Y.; Chen, Y.; et al. Recent progress of two-dimensional thermoelectric materials. *Nano Micro Lett.* **2020**, *12*, 36. https://doi.org/10.1007/s40820-020-0374-x.
91. Wang, Y.; Chen, S.Y.; Ruan, X.L. Tunable thermal rectification in graphene nanoribbons through defect engineering: A molecular dynamics study. *Appl. Phys. Lett.* **2012**, *100*, 163101. https://doi.org/10.1063/1.3703756.
92. Pei, Q.X.; Zhang, Y.W.; Sha, Z.D.; et al. Carbon isotope doping induced interfacial thermal resistance and thermal rectification in graphene. *Appl. Phys. Lett.* **2012**, *100*, 101901. https://doi.org/10.1063/1.3692173.
93. Rajabpour, A.; Allaei, S.M.V.; Kowsary, F. Interface thermal resistance and thermal rectification in hybrid graphene-graphane nanoribbons: A nonequilibrium molecular dynamics study. *Appl. Phys. Lett.* **2011**, *99*, 051917. https://doi.org/10.1063/1.3622480.
94. Yuan, K.P.; Sun, M.M.; Wang, Z.L.; et al. Tunable thermal rectification in silicon-functionalized graphene nanoribbons by molecular dynamics simulation. *Int. J. Therm. Sci.* **2015**, *98*, 24–31. https://doi.org/10.1016/j.ijthermalsci.2015.07.004.
95. Gunawardana, K.; Mullen, K.; Hu, J.N.; et al. Tunable thermal transport and thermal rectification in strained graphene nanoribbons. *Phys. Rev. B* **2012**, *85*, 245417. https://doi.org/10.1103/PhysRevB.85.245417.
96. Sadeghi, M.M.; Huang, Y.; Lian, C.; et al. Tunable electron-flexural phonon interaction in graphene heterostructures. *Nature* **2023**, *617*, 282–286. https://doi.org/10.1038/s41586-023-05879-y.
97. Pan, Y.; Caruso, F. Strain-induced activation of chiral-phonon emission in monolayer WS_2. *NPJ 2D Mater. Appl.* **2024**, *8*, 42. https://doi.org/10.1038/s41699-024-00479-4.
98. Feng, N.; Tian, Y.; Han, J.; et al. Phonon-phonon interaction assisted electron-hole recombination in WSe_2/hBN van der Waals heterostructure. *J. Appl. Phys.* **2021**, *130*, 205708. https://doi.org/10.1063/5.0070269.
99. Chiritescu, C.; Cahill, D.G.; Nguyen, N.; et al. Ultralow thermal conductivity in disordered, layered WSe_2 crystals. *Science* **2007**, *315*, 351–353. https://doi.org/10.1126/science.1136494.
100. Chen, X.K.; Pang, M.; Chen, T.; et al. Thermal rectification in asymmetric graphene/hexagonal boron nitride van der waals heterostructures. *ACS Appl. Mater. Interfaces* **2020**, *12*, 15517–15526. https://doi.org/10.1021/acsami.9b22498.
101. Ding, W.Y.; Ong, Z.Y.; An, M.; et al. Optimally suppressed phonon tunneling in van der waals graphene-WS_2 heterostructure

with ultralow thermal conductivity. *Nano Lett.* **2024**, *24*, 13754–13759. https://doi.org/10.1021/acs.nanolett.4c03930.
102. Chen, X.K.; Xie, Z.X.; Zhou, W.X.; et al. Thermal rectification and negative differential thermal resistance behaviors in graphene/hexagonal boron nitride heterojunction. *Carbon* **2016**, *100*, 492–500. https://doi.org/10.1016/j.carbon.2016.01.045.
103. Vaziri, S.; Yalon, E.; Rojo, M.M.; et al. Ultrahigh thermal isolation across heterogeneously layered two-dimensional materials. *Sci. Adv.* **2019**, *5*, eaax1325. https://doi.org/10.1126/sciadv.aax1325.
104. Jia, P.Z.; Zeng, Y.J.; Wu, D.; et al. Excellent thermoelectric performance induced by interface effect in MoS_2/$MoSe_2$ van der Waals heterostructure. *J. Phys.-Condes. Matter* **2020**, *32*, 055302. https://doi.org/10.1088/1361-648X/ab4cab.
105. Jia, P.Z.; Xie, J.P.; Chen, X.K.; et al. Recent progress of two-dimensional heterostructures for thermoelectric applications. *J. Phys.-Condes. Matter* **2023**, *35*, 073001. https://doi.org/10.1088/1361-648X/aca8e4.
106. Sun, W.F.; Xue, S.J.; Jiang, J. Molecular dynamics study on the thermal conductivity and ballistic resistance of twisted graphene. *Comput. Mater. Sci.* **2023**, *229*, 112436. https://doi.org/10.1016/j.commatsci.2023.112436.
107. Havener, R.W.; Zhuang, H.L.; Brown, L.; et al. Angle-resolved Raman imaging of inter layer rotations and interactions in twisted bilayer graphene. *Nano Lett.* **2012**, *12*, 3162–3167. https://doi.org/10.1021/nl301137k.
108. Park, J.M.; Cao, Y.; Watanabe, K.; et al. Tunable strongly coupled superconductivity in magic-angle twisted trilayer graphene. *Nature* **2021**, *590*, 249–255. https://doi.org/10.1038/s41586-021-03192-0.
109. Kim, H.; Choi, Y.; Lewandowski, C.; et al. Evidence for unconventional superconductivity in twisted trilayer graphene. *Nature* **2022**, *606*, 494–500. https://doi.org/10.1038/s41586-022-04715-z.
110. Li, H.Y.; Ying, H.; Chen, X.P.; et al. Thermal conductivity of twisted bilayer graphene. *Nanoscale* **2014**, *6*, 13402–13408. https://doi.org/10.1039/c4nr04455j.
111. Chen, M.Y.; Lin, X.; Dinh, T.H.; et al. Configurable phonon polaritons in twisted α-MoO_3. *Nat. Mater.* **2020**, *19*, 1307–1311. https://doi.org/10.1038/s41563-020-0732-6.
112. Qin, Z.H.; Dai, L.Y.; Li, M.; et al. Moiré pattern controlled phonon polarizer based on twisted graphene. *Adv. Mater.* **2024**, *36*, 2312176. https://doi.org/10.1002/adma.202312176.
113. Wu, F.C.; MacDonald, A.H.; Martin, I. Theory of phonon-mediated superconductivity in twisted bilayer graphene. *Phys. Rev. Lett.* **2018**, *121*, 257001. https://doi.org/10.1103/PhysRevLett.121.257001.
114. Liu, Y.Z.; Chen, X.B.; Xu, Y. Topological phononics: From fundamental models to real materials. *Adv. Funct. Mater.* **2020**, *30*, 1904784. https://doi.org/10.1002/adfm.201904784.
115. Hasan, M.Z.; Kane, C.L. Colloquium: Topological insulators. *Rev. Mod. Phys.* **2010**, *82*, 3045–3067. https://doi.org/10.1103/RevModPhys.82.3045.
116. Lukyanchuk, I.; Vinokur, V.M.; Rydh, A.; et al. Rayleigh instability of confined vortex droplets in critical superconductors. *Nat. Phys.* **2015**, *11*, 21–25. https://doi.org/10.1038/nphys3146.
117. Cheng, Y.; Wu, X.; Zhang, Z.J.; et al. Thermo-mechanical correlation in two-dimensional materials. *Nanoscale* **2021**, *13*, 1425–1442. https://doi.org/10.1039/d0nr06824a.
118. Zhu, H.Y.; Yi, J.; Li, M.Y.; et al. Observation of chiral phonons. *Science* **2018**, *359*, 579–581. https://doi.org/10.1126/science.aar2711.
119. Luo, J.M.; Li, S.Y.; Ye, Z.P.; et al. Evidence for topological magnon-phonon hybridization in a 2d antiferromagnet down to the monolayer limit. *Nano Lett.* **2023**, *23*, 2023–2030. https://doi.org/10.1021/acs.nanolett.3c00351.
120. Bours, L.; Sothmann, B.; Carrega, M.; et al. Phase-tunable thermal rectification in the topological SQUIPT. *Phys. Rev. Appl.* **2019**, *11*, 044073. https://doi.org/10.1103/PhysRevApplied.11.044073.
121. Xu, Y.F.; Vergniory, M.G.; Ma, D.S.; et al. Catalog of topological phonon materials. *Science* **2024**, *384*, eadf8458. https://doi.org/10.1126/science.adf8458.
122. Jin, X.; Ma, D.S.; Yu, P.; et al. Strain-driven phonon topological phase transition impedes thermal transport in titanium monoxide. *Cell Rep. Phys. Sci.* **2024**, *5*, 101895. https://doi.org/10.1016/j.xcrp.2024.101895.
123. Wang, Q.Q.; Li, S.; Zhu, J.J.; et al. Chiral phonons in lattices with C4 symmetry. *Phys. Rev. B* **2022**, *105*, 104301. https://doi.org/10.1103/PhysRevB.105.104301.
124. Lu, Q.Y.; Huberman, S.; Zhang, H.T.; et al. Bi-directional tuning of thermal transport in $SrCoO_x$ with electrochemically induced phase transitions. *Nat. Mater.* **2020**, *19*, 655–662. https://doi.org/10.1038/s41563-020-0612-0.
125. Saeedi, A.; Akizi, F.Y.; Khademsadr, S.; et al. Thermal rectification of a single-wall carbon nanotube: A molecular dynamics study. *Solid. State Commun.* **2014**, *179*, 54–58. https://doi.org/10.1016/j.ssc.2013.10.026.
126. Budaev, B.V.; Bogy, D.B. Thermal rectification in inhomogeneous nanotubes. *Appl. Phys. Lett.* **2016**, *109*, 231905.
127. Lei, G.P.; Cheng, H.Y.; Liu, H.T.; et al. Thermal rectification in asymmetric graphyne nanoribbons: A nonequilibrium molecular dynamics study. *Mater. Lett.* **2017**, *189*, 101–103. https://doi.org/10.1016/j.matlet.2016.11.092.
128. Sandonas, L.M.; Gutierrez, R.; Dianat, A.; et al. Engineering thermal rectification in MoS_2 nanoribbons: A non-equilibrium molecular dynamics study. *RSC Adv.* **2015**, *5*, 54345–54351. https://doi.org/10.1039/c5ra05733g.
129. Starr, C. The copper oxide rectifier. *J. Appl. Phys.* **1936**, *7*, 15–19. https://doi.org/10.1063/1.1745338.
130. Zhao, S.Y.; Zhou, Y.H.; Wang, H.D. Review of thermal rectification experiments and theoretical calculations in 2D

materials. *Int. J. Heat. Mass. Transfer* **2022**, *195*, 123218. https://doi.org/10.1016/j.ijheatmasstransfer.2022.123218.

131. Hu, J.N.; Wang, Y.; Vallabhaneni, A.; et al. Nonlinear thermal transport and negative differential thermal conductance in graphene nanoribbons. *Appl. Phys. Lett.* **2011**, *99*, 113101. https://doi.org/10.1063/1.3630026.
132. Chen, M.E.; Rojo, M.M.; Lian, F.F.; et al. Graphene-based electromechanical thermal switches. *2D Mater.* **2021**, *8*, 035055. https://doi.org/10.1088/2053-1583/abf08e.
133. Zhong, W.R.; Zheng, D.Q.; Hu, B.B. Thermal control in graphene nanoribbons: Thermal valve, thermal switch and thermal amplifier. *Nanoscale* **2012**, *4*, 5217–5220. https://doi.org/10.1039/c2nr30634d.
134. Lim, M.; Kim, H.D.; Shim, H.C.; et al. Optically transparent and infrared tunable flexible camouflage device. *Nano Energy* **2024**, *131*, 110189. https://doi.org/10.1016/j.nanoen.2024.110189.
135. Bianco, V.; De Rosa, M.; Vafai, K. Phase-change materials for thermal management of electronic devices. *Appl. Therm. Eng.* **2022**, *214*, 118839. https://doi.org/10.1016/j.applthermaleng.2022.118839.
136. Lawag, R.A.; Ali, H.M. Phase change materials for thermal management and energy storage: A review. *J. Energy Storage* **2022**, *55*, 105602. https://doi.org/10.1016/j.est.2022.105602.
137. Meng, T.; Sun, Y.W.; Tong, C.; et al. Solid-state thermal memory of temperature-responsive polymer induced by hydrogen bonds. *Nano Lett.* **2021**, *21*, 3843–3848. https://doi.org/10.1021/acs.nanolett.1c00289.
138. Suk, J.W.; Kirk, K.; Hao, Y.F.; et al. Thermoacoustic sound generation from monolayer graphene for transparent and flexible sound sources. *Adv. Mater.* **2012**, *24*, 6342–6347. https://doi.org/10.1002/adma.201201782.
139. Fan, C.Z.; Gao, Y.; Huang, J.P. Shaped graded materials with an apparent negative thermal conductivity. *Appl. Phys. Lett.* **2008**, *92*, 251907. https://doi.org/10.1063/1.2951600.
140. Han, T.C.; Bai, X.; Thong, J.T.L.; et al. Full control and manipulation of heat signatures: Cloaking, camouflage and thermal metamaterials. *Adv. Mater.* **2014**, *26*, 1731–1734. https://doi.org/10.1002/adma.201304448.
141. Wang, Y.; Huang, H.X.; Ruan, X.L. Decomposition of coherent and incoherent phonon conduction in superlattices and random multilayers. *Phys. Rev. B* **2014**, *90*, 165406. https://doi.org/10.1103/PhysRevB.90.165406.
142. Lee, S.; Broido, D.; Esfarjani, K.; et al. Hydrodynamic phonon transport in suspended graphene. *Nat. Commun.* **2015**, *6*, 6290. https://doi.org/10.1038/ncomms7290.
143. Li, M.; Dai, L.Y.; Hu, Y.J. Machine learning for harnessing thermal energy: From materials discovery to system optimization. *ACS Energy Lett.* **2022**, *7*, 3204–3226. https://doi.org/10.1021/acsenergylett.2c01836.
144. Ji, Q.X.; Qi, Y.C.; Liu, C.W.; et al. Design of thermal cloaks with isotropic materials based on machine learning. *Int. J. Heat. Mass. Transfer* **2022**, *189*, 122716. https://doi.org/10.1016/j.ijheatmasstransfer.2022.122716.
145. Ji, Q.X.; Chen, X.Y.; Liang, J.; et al. Deep learning based design of thermal metadevices. *Int. J. Heat. Mass. Transfer* **2022**, *196*, 123149. https://doi.org/10.1016/j.ijheatmasstransfer.2022.123149.